JACS
JOURNAL OF THE AMERICAN CHEMICAL SOCIETY
pubs.acs.org/JACS
Article

High Triplet Energy Iridium(III) Isocyanoborato Complex for Photochemical Upconversion, Photoredox and Energy Transfer Catalysis

Lucius Schmid, Felix Glaser, Raoul Schaer, and Oliver S. Wenger*

Cite This: J. Am. Chem. Soc. 2022, 144, 963−976
Read Online
ACCESS | Metrics & More | Article Recommendations | Supporting Information

ABSTRACT: Cyclometalated Ir(III) complexes are often chosen as catalysts for challenging photoredox and triplet−triplet-energy-transfer (TTET) catalyzed reactions, and they are of interest for upconversion into the ultraviolet spectral range. However, the triplet energies of commonly employed Ir(III) photosensitizers are typically limited to values around 2.5−2.75 eV. Here, we report on a new Ir(III) luminophore, with an unusually high triplet energy near 3.0 eV owing to the modification of a previously reported Ir(III) complex with isocyanoborato ligands. Compared to a nonborylated cyanido precursor complex, the introduction of $B(C_6F_5)_3$ units in the second coordination sphere results in substantially improved photophysical properties, in particular a high luminescence quantum yield (0.87) and a long excited-state lifetime (13.0 μs), in addition to the high triplet energy. These favorable properties (including good long-term photostability) facilitate exceptionally challenging organic triplet photoreactions and (sensitized) triplet−triplet annihilation upconversion to a fluorescent singlet excited state beyond 4 eV, unusually deep in the ultraviolet region. The new Ir(III) complex photocatalyzes a sigmatropic shift and [2 + 2] cycloaddition reactions that are unattainable with common transition metal-based photosensitizers. In the presence of a sacrificial electron donor, it furthermore is applicable to demanding photoreductions, including dehalogenations, detosylations, and the degradation of a lignin model substrate. Our study demonstrates how rational ligand design of transition-metal complexes (including underexplored second coordination sphere effects) can be used to enhance their photophysical properties and thereby broaden their application potential in solar energy conversion and synthetic photochemistry.

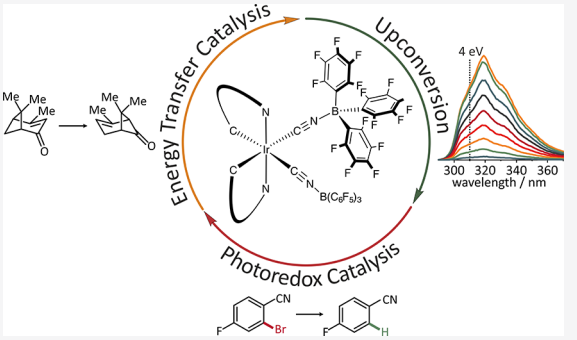

INTRODUCTION

Triplet−triplet energy transfer (TTET) catalysis has become an important tool of organic-synthetic photochemistry, because many reactions rely on triplet excited states that are difficult to access directly.[1] TTET catalysis proceeds via sensitization of triplet-excited states of organic[1,2] and inorganic[3−6] substrates without the need for excitation of their singlet-excited states, thereby allowing for milder reaction conditions (using visible instead of UV excitation light) and higher selectivity. Similarly, triplet−triplet annihilation upconversion crucially relies on triplet sensitization.[7,8] The triplet energy of the photosensitizer is a limiting factor for both types of applications, TTET catalysis, and upconversion.

Prominent examples of TTET catalyzed organic reactions include *E*/*Z* isomerizations,[9−14] cycloadditions,[15−25] the disulfide-ene reaction,[26] C-(sp^3)−H methylations,[27] and the photocatalyzed Paternò−Büchi reaction.[28,29] The scope of substrates is typically dictated by the triplet energy of the available photosensitizers, and the development of photocatalysts with higher triplet energies is desirable to enable more challenging substrates or even new reactions. Transition metal complexes are widely used as TTET and photoredox catalysts,[30] due to their high intersystem crossing efficiencies that usually lead to quantitative population of triplet excited states, as well as the tunability of their photophysical properties and their photostability.[31−33] Though earth-abundant first- and second-row transition metal complexes become increasingly popular,[34−36] so far mostly precious Ru(II)- and Ir(III)-based photocatalysts have been employed, with cyclometalated Ir(III) complexes representing a particularly popular choice for reactions requiring comparatively high triplet energies.[37,38] However, most commonly used Ir(III) photosensitizers do not exceed triplet energies of 2.7 eV,[1] and the metal-based TTET catalyst with the highest triplet energy that is typically employed is [Ir(dFppy)$_3$] (dFppy = 2-(2,4-difluorophenyl)-

Received: November 4, 2021
Published: January 5, 2022

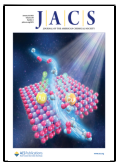

pyridine), with a triplet energy of 2.75 eV (Figure 1a).[2,31,39−41] Other metal complexes also exhibit high triplet energies (up to 3.26 eV),[42−46] but it seems that their performance in TTET catalysis has not yet been explored. Very recently, a tris-cyclometalated Ir(III) complex with a triplet energy of 3.18 eV and its application in a De Mayo type reaction was reported.[47] Organic, nonmetal based photosensitizers with high triplet energies (Figure 1b) include thioxanthone (E_T = 2.75 eV), benzophenone (E_T = 2.98 eV), and acetophenone (E_T = 3.21 eV).[1] However, such ketone-based sensitizers can suffer from some severe drawbacks: often, substoichiometric amounts of the catalyst are necessary, and their triplet-excited states can be susceptible to side reactions and increased photodegradation.[1,19] This class of sensitizers furthermore has low extinction coefficients at readily accessible excitation wavelengths (for benzophenone the molar extinction coefficient at 346 nm is only 60 M^{-1} cm^{-1}),[48] thereby leading to inefficient light absorption unless very short wavelength excitation light is used. Consequently, the development of metal-based TTET catalysts with high triplet energies represents an attractive research target. Furthermore, such compounds may permit sensitized triplet−triplet annihilation upconversion to exceptionally high energies, resulting in delayed fluorescence in the difficult to access ultraviolet B region.

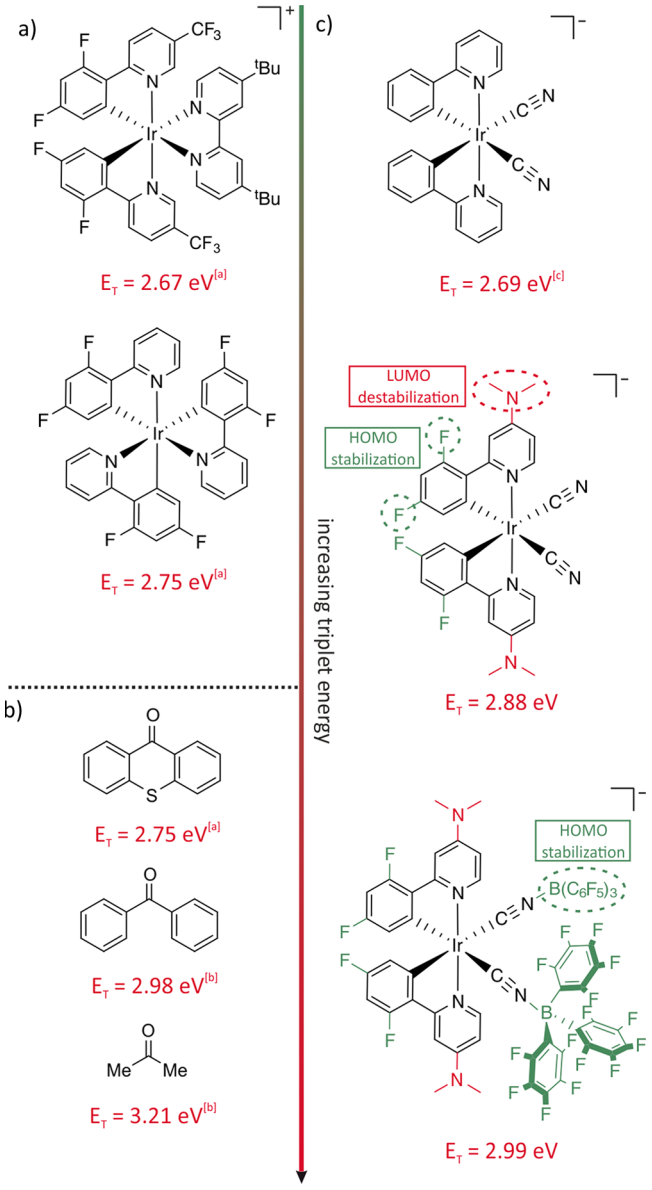

Figure 1. Chemical structures and triplet energies of important metal-based (a) and organic (b) photosensitizers. (c) Chemical structures of $[Ir(ppy)_2(CN)_2]^-$ (top), $[Ir(dFN(Me)_2ppy)_2(CN)_2]^-$ (middle), and $[Ir(dFN(Me)_2ppy)_2(BCF)_2]^-$ (bottom) and the key effects of the individual ligand substituents. [a]: from ref 2. [b]: from ref 49. [c]: from ref 50. The organic photosensitizers shown in (b) require excitation in the ultraviolet (UV) spectral range.

Here, we present a detailed photophysical and photochemical study of a new heteroleptic Ir(III) complex obtained via the borylation of a cyclometalated Ir(III) cyanido precursor complex, to benefit from the favorable influences of the resulting isocyanoborato ligands.[51−65] Starting from the known $[Ir(dFN(Me)_2ppy)_2(CN)_2]^-$ complex ((dFN(Me)$_2$ppy) = 2-(2,4-difluorophenyl)-*N*,*N*-dimethylpyridin-4-amine), reaction with $B(C_6F_5)_3$ gave $[Ir(dFN(Me)_2ppy)_2(BCF)_2]^-$ (Figure 1c, BCF = $CNB(C_6F_5)_3$). This new complex exhibits an exceptionally high triplet energy of 2.99 eV that allows for the sensitization of organic substrates that were hitherto not easily amenable by (known) metal-based photosensitizers. Though there have been several detailed reports on the photophysical and electrochemical properties of isocyanoborato complexes with different metals,[51−64] their photochemical properties, as well as their applications in TTET catalysis and photochemical upconversion, have remained underexplored so far.[65]

In addition to unusually challenging applications in TTET catalysis, the new complex permits sensitized triplet−triplet-annihilation upconversion (sTTA-UC) into the UV−B region. There have been numerous reports on visible/near-infrared to visible[66−74] as well as a few visible to UV[75−80] upconversion systems, but only a very small number of them can provide emission below 350 nm.[81−84] With $[Ir(dFN(Me)_2ppy)_2(BCF)_2]^-$ as sensitizer and 4,4′-di-*tert*-butyl-biphenyl as annihilator, photochemical upconversion to a fluorescent singlet excited state beyond 4 eV becomes possible. Upconversion this far into the ultraviolet range has only recently been reported[85] and could potentially represent an alternative way to generating light for which, traditionally, mercury lamps have been used. The good photorobustness of the new Ir(III) complex under triplet sensitization conditions is encouraging in this regard.

Lastly, we found that excitation of $[Ir(dFN(Me)_2ppy)_2(BCF)_2]^-$ in the presence of excess tertiary alkyl amine leads to its one-electron reduced form, which is a very strong reductant featuring a redox potential of −2.42 V vs SCE. This permits efficient reductive dehalogenations of activated aryl bromides and chlorides, detosylation reactions, and the reductive C_α−O bond cleavage in a small molecule resembling lignin.

RESULTS AND DISCUSSION

Ligand and Complex Design. The electronic structure of Ir(III) complexes with phenylpyridine ligands can be tuned by the introduction of suitable electron-withdrawing or -donating substituents on the phenyl and the pyridine moiety.[32,86−88] Aiming at an increased triplet energy and based on previous work,[45] we targeted the $[Ir(dFN(Me)_2ppy)_2(BCF)_2]^-$ complex (Figure 1c, bottom), in which *N*,*N*-dimethylamino groups at the 4-position of the pyridine moiety destabilize the lowest unoccupied molecular orbital (LUMO), whereas fluoro

https://doi.org/10.1021/jacs.1c11667
J. Am. Chem. Soc. 2022, 144, 963−976

substituents at the 4- and 6-positions of the phenyl ring stabilize the highest occupied molecular orbital (HOMO). These combined effects lead to a triplet energy of 2.88 eV in the known $[Ir(dFN(Me)_2ppy)_2(CN)_2]^-$ complex (Figure 1c, middle),[45] and in order to increase the energy of the photoactive triplet excited state even further, we attached the strongly Lewis acidic $B(C_6F_5)_3$ moiety to both CN^- ligands. This results in an additional stabilization of the metal-based t_{2g}-like HOMO.[51] Combining the effects of the *N*,*N*-dimethylamino and fluoro substituents at the ppy-chelators with $B(C_6F_5)_3$ at the cyanido ligands results in a triplet energy (E_T) of 2.99 eV, which is ca. 0.30 eV higher than in the unsubstituted $[Ir(ppy)_2(CN)_2]^-$ complex (Figure 1c, top).[50]

Synthesis, Infrared Spectroscopy, and Electrochemistry. The precursor compound $[TBA][Ir(dFN(Me)_2ppy)_2(CN)_2]$ (TBA = tetra-*n*-butylammonium) was synthesized in four steps following published procedures, but some improvements to the reported syntheses were made (see SI, page S4 for experimental details).[44,45] The cyanoborylated $[TBA][Ir(dFN(Me)_2ppy)_2(BCF)_2]$ compound was obtained by reacting $[TBA][Ir(dFN(Me)_2ppy)_2(CN)_2]$ with 2.2 equiv of $B(C_6F_5)_3$ in dry and degassed CH_2Cl_2 and was characterized by ^1H, ^{19}F, ^{11}B, and ^{13}C NMR spectroscopy as well as by elemental analysis (EA), infrared (IR) spectroscopy, and high-resolution mass spectrometry (HRMS).

In the IR-spectrum of nonborylated $[Ir(dFN(Me)_2ppy)_2(CN)_2]^-$, two C≡N bands are observed at 2100 and 2091 cm^{-1}, and upon attachment of $B(C_6F_5)_3$ these bands are shifted to 2195 and 2180 cm^{-1} in $[Ir(dFN(Me)_2ppy)_2(BCF)_2]^-$ (Figure S21). This ca. 100 cm^{-1} blue shift of the C≡N stretch frequencies is commonly observed upon the borylation of cyanido precursor complexes and is due to the electron-withdrawing nature of the $B(C_6F_5)_3$ group, which lowers the energy of the relevant C≡N π-bonding orbitals, resulting in a stronger C≡N bond.[64]

In the cyclic (CV) and differential pulse voltammograms (DPV) of $[TBA][Ir(dFN(Me)_2ppy)_2(BCF)_2]$ recorded in dry and deaerated CH_3CN, a ligand-based reduction at −2.42 V vs SCE (E^{red}) and a metal-centered oxidation feature at 1.40 V vs SCE (E^{ox}) are observed (Figure 2). The corresponding oxidation of $[Ir(dFN(Me)_2ppy)_2(CN)_2]^-$ takes place at a substantially less positive potential of 0.97 V vs SCE (Figure S22), indicating that borylation of the two cyanido ligands entails a stabilization of the metal-centered t_{2g}-like HOMOs by ca. 0.43 eV, an effect which is commonly observed upon the borylation of heteroleptic Ir(III) cyanido complexes.[51] Similarly, the reduction of $[Ir(dFN(Me)_2ppy)_2(BCF)_2]^-$ at −2.42 V vs SCE is at a less negative potential than in $[Ir(dFN(Me)_2(ppy)_2(CN)_2]^-$ (−2.59 V vs SCE), signaling that the ligand-based LUMO has been stabilized by ca. 0.17 eV. Since the $B(C_6F_5)_3$ units are attached remotely at the cyanido ligands, borylation acts less strongly on the essentially ppy-centered LUMO than on the largely metal-based HOMO. The combination of both borylation effects is expected to lead to an increase of the energy of the photoactive excited state by ca. 0.26 eV, based on these electrochemical data.

The singly reduced $[Ir(dFN(Me)_2ppy)_2(BCF)_2]^{2-}$ species with its oxidation potential of −2.42 V vs SCE should be a powerful reductant, and this is confirmed by the photochemical studies discussed further below.

Photophysical Properties. The UV−vis absorption spectrum of $[TBA][Ir(dFN(Me)_2ppy)_2(BCF)_2]$ (green solid trace in Figure 3) shows $\pi-\pi^*$ transitions (220−310 nm) as well as mixed metal-to-ligand-charge-transfer/intraligand (MLCT/IL) transitions (centered at 328 nm).[45,51] Following 355 nm excitation of a 10^{-5} M deaerated CH_3CN solution of $[TBA][Ir(dFN(Me)_2ppy)_2(BCF)_2]$, a structured emission band centered at 448 nm is detectable (dashed red trace in Figure 3). Both the MLCT/IL UV−vis absorption and the emission band are blue-shifted by ca. 0.12 eV compared to the parent cyanido complex (Figure S23) due to the Lewis acidic nature of $B(C_6F_5)_3$ (Table 1), which is lower than the value of

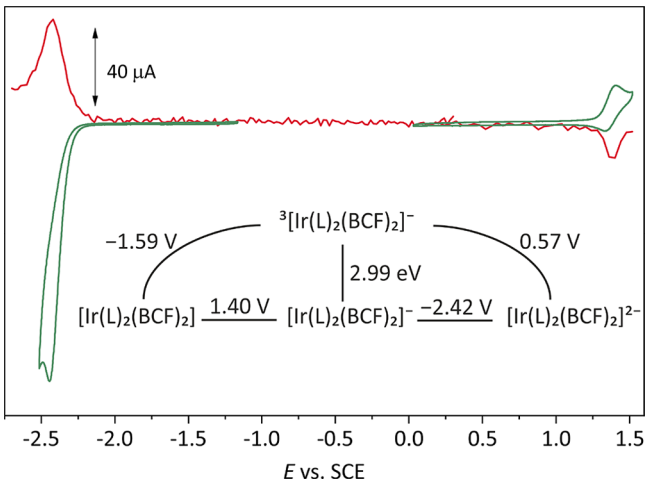

Figure 2. Main plot: cyclic voltammogram (CV, green) and differential pulse voltammogram (DPV, red) of 1 mM $[TBA][Ir(L)_2(BCF)_2]$ in dry, deaerated CH_3CN with 0.1 M $[TBA][PF_6]$ as supporting electrolyte. L = $(dFN(Me)_2ppy)_2$. For the CV, the scan rate was 0.1 V/s; for the DPV, the step height was 20 mV, the pulse height was 40 mV, the pulse width was 90 ms, and the step width was 100 ms. Inset: Latimer diagram derived from the electrochemical measurements presented in the main plot and the energy of the photoactive excited state as determined by the spectroscopic studies below. Redox potentials in the inset are referenced to the saturated calomel electrode (SCE).

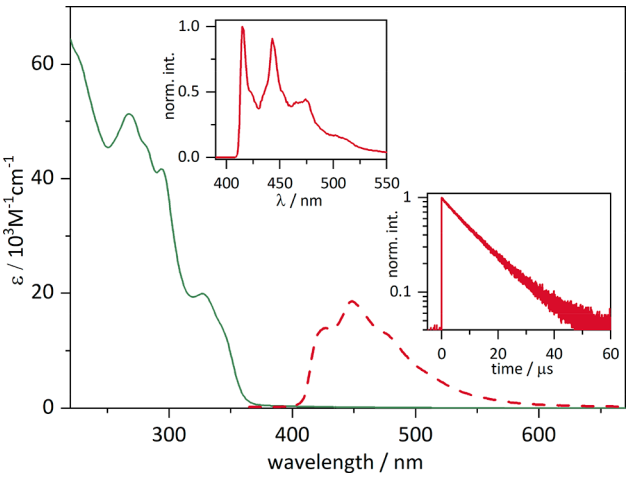

Figure 3. Main plot: UV−vis absorption (green line) and luminescence (dashed red line) spectra of 10^{-5} M $[TBA][Ir(dFN(Me)_2ppy)_2(BCF)_2]$ recorded in dry, deaerated CH_3CN at 293 K. Left inset: luminescence spectrum of $[TBA][Ir(dFN(Me)_2ppy)_2(BCF)_2]$ recorded in 2-methyl-THF at 77 K. Right inset: luminescence decay of 10^{-5} M $[TBA][Ir(dFN(Me)_2ppy)_2(BCF)_2]$ in dry, deaerated CH_3CN at 293 K after excitation at 355 nm with laser pulses of ∼10 ns duration. For the steady-state luminescence spectra, excitation occurred at 350 nm.

https://doi.org/10.1021/jacs.1c11667
J. Am. Chem. Soc. 2022, 144, 963−976

Table 1. Summary of the Photophysical[a] and Electrochemical[b] Properties of [TBA][Ir(L)$_2$(BCF)$_2$] and [TBA][Ir(L)$_2$(CN)$_2$] as well as Literature Values of the Two Reference Compounds Benzophenone and [Ir(dFppy)$_3$] (L = (dFN(Me)$_2$ppy))[c]

	$\lambda_{max,\ abs,\ MLCT/IL}$ (ε)/ (nm (M^{-1} cm^{-1}))	$\varepsilon_{415\ nm}$ (M^{-1} cm^{-1})	$\lambda_{max,\ em}$ (nm)	τ_0 (μs)	E_T (eV)	Φ_{lum} (%)	E^{red} (V vs SCE)	E^{ox} (V vs SCE)
[Ir(L)$_2$(BCF)$_2$]$^-$	328 (20,000)	260	448	13.0	2.99[d]	87	−2.42	1.40
[Ir(L)$_2$(CN)$_2$]$^-$	343 (12,500)	520	468	2.8	2.88[d]	64	−2.59	0.97
Benzophenone	–	0[89]	451[90]	50.0[49]	2.98[1]	1.3[90]	–	–
[Ir(dFppy)$_3$]	–	2,000[91]	476[92]	1.6[31]	2.75[2]	43[86]	−1.87[31]	0.94[31]

[a]Photophysical data were obtained in dry, deaerated CH_3CN at 293 K. [b]Electrochemical data were obtained in dry, deaerated CH_3CN at room temperature with 0.1 M [TBA][PF_6] as supporting electrolyte. [c]$\lambda_{max,\ abs,\ MLCT/IL}$ is the wavelength of the lowest-energy absorption band maximum (reported along with the molar extinction coefficient (ε) at that wavelength), $\varepsilon_{415\ nm}$ is the molar extinction coefficient at 415 nm, and $\lambda_{max,\ em}$ is the wavelength of the emission band maximum. All other abbreviations used in this table are defined in the text. [d]Triplet energies (E_T) were obtained from 77 K measurements in 2-methyl-THF.

0.26 eV expected on the basis of the electrochemical data discussed above.

Compared to the blue shifts of the absorption and emission bands observed upon borylation of Ru(II) polypyridyl cyanido complexes (ca. 0.5 eV from [Ru(bpy)$_2$(CN)$_2$] to [Ru(bpy)$_2$(BCF)$_2$], bpy = 2,2′-bipyridine),[65] this effect is rather modest, and we attribute this to the somewhat different nature of the emissive excited states of Ru(II) polypyridyls compared to cyclometalated Ir(III) complexes: In the respective Ru(II) complexes, the emissive state is a relatively clean MLCT, while in cyclometalated Ir(III) compounds it has mixed MLCT/IL character.[93−96] As B(C_6F_5)$_3$ mainly stabilizes the metal-centered HOMO, but due to its attachment at the cyanido ligands acts much less on the ppy-localized π and π^* orbitals, the increase in energy of the photoactive excited state is larger for clean MLCT emitters compared to mixed MLCT/IL luminophores.[51] This effect is also observed upon methylation of the [Ru(bpy)(CN)$_4$]$^{2-}$ complex to obtain [Ru(bpy)(CNMe)$_4$]$^{2+}$, leading to a relatively large increase in triplet energy of ∼0.5 eV.[97]

Despite the substantially blue-shifted MLCT/IL excited state of [TBA][Ir(dFN(Me)$_2$ppy)$_2$(BCF)$_2$], excitation with a commercial 415 nm LED remains feasible due to the tailing of its lowest absorption band into the visible region, as well as the fact that the spectral output of such an LED extends to roughly 390 nm (Figure S28). The molar extinction coefficient of [TBA][Ir(dFN(Me)$_2$ppy)$_2$(BCF)$_2$] at 415 nm in CH_3CN is 260 M^{-1} cm^{-1}, which is sufficient for the application of this complex in energy transfer and photoredox catalysis, as illustrated in the following sections. For comparison, the well-known organic triplet sensitizer benzophenone does not absorb significantly at 415 nm, and therefore, much higher energy photons are typically needed for its excitation (Table 1).

77 K luminescence measurements of [TBA][Ir(dFN(Me)$_2$ppy)$_2$(BCF)$_2$] in 2-methyl-THF reveal a triplet energy of 2.99 eV, as determined from the highest-energy emission peak at 415 nm (left inset in Figure 3). The emission band at this temperature is highly structured with a vibrational progression in a 1500 cm^{-1} mode, indicating significant intraligand character of the photoluminescence under these conditions. This fine structure is not observed in the nonborylated [Ir(dFN(Me)$_2$ppy)$_2$(CN)$_2$]$^-$ parent complex (Figure S23). The inherent excited-state lifetime (τ_0) of [Ir(dFN(Me)$_2$ppy)$_2$(CN)$_2$]$^-$ in dry and deaerated CH_3CN at 293 K is 2.8 μs, and this value is elongated by a factor of ∼4.5 to 13.0 μs in [Ir(dFN(Me)$_2$ppy)$_2$(BCF)$_2$]$^-$ (right inset in Figure 3). Excited-state lifetime elongation is typically observed upon borylation of cyanido complexes with the 5d metals Ir(III),[51] Re(I)[52−54,56] and Os(II),[57] and here this effect might be further aided by increased ^{3}IL character. The elongation of the luminescence lifetime is furthermore in line with the energy gap law, which predicts a decrease in nonradiative relaxation with increasing excited-state energy.[98] This moreover results in an improved luminescence quantum yield (Φ_{lum}) of 0.87 for [Ir(dFN(Me)$_2$ppy)$_2$(BCF)$_2$]$^-$ in deaerated CH_3CN at 293 K compared to 0.64 for [Ir(dFN(Me)$_2$ppy$_2$(CN)$_2$]$^-$ under identical conditions.

In the transient UV−vis absorption (TA) spectra of both [TBA][Ir(dFN(Me)$_2$ppy)$_2$(CN)$_2$] (Figure S24) and [TBA][Ir(dFN(Me)$_2$ppy)$_2$(BCF)$_2$] (Figure S26), an excited-state absorption (ESA) band with a maximum at 400 nm, tentatively attributable to the reduced dFN(Me)$_2$ppy ligand, is observed. In both complexes, this ESA band exhibits the same lifetime as the emission of the respective complex (2.8 μs for [Ir(dFN(Me)$_2$ppy)$_2$(CN)$_2$]$^-$ and 13.0 μs for [Ir(dFN(Me)$_2$ppy)$_2$(BCF)$_2$]$^-$), confirming that the same photoexcited species are probed by luminescence and TA.

Energy Transfer Catalysis. With its exceptionally high triplet energy of 2.99 eV, the new Ir(III) isocyanoborato complex is a very promising candidate for TTET catalysis. In a first test reaction, we investigated the intramolecular [2 + 2] cycloaddition of norbornadiene to quadricyclane (Figure 4a). This reaction is of interest in the context of solar energy conversion due to the ability of quadricyclane to store chemical energy and release it on demand.[99−102] However, a disadvantage of this system is that norbornadiene does not absorb significantly in the visible region and furthermore it has a comparatively high triplet energy of 2.7 eV. In our experiments, 0.3 mol % [Ir(dFN(Me)$_2$ppy)$_2$(BCF)$_2$]$^-$ catalyzed the conversion of norbornadiene to quadricyclane efficiently in deaerated CD_3CN upon irradiation with the above-mentioned 415 nm LED and gave a 99% NMR-yield after a reaction time of 1 h (Figure 4a). We estimate the photochemical quantum yield (Φ_{PC}) for this reaction, defined here as quadricyclane molecules formed per number of absorbed photons, to ∼0.3 (see SI, page S26 for details).

When lowering the catalyst loading to 0.02 mol %, an NMR-yield of 92% remained achievable over 8 h, corresponding to a turnover number (TON) > 4500. The comparatively long photoirradiation time and high TON point to the good photostability of [Ir(dFN(Me)$_2$ppy)$_2$(BCF)$_2$]$^-$ under photocatalytic conditions, and this important aspect will be explored in detail below. Even though the conversion of norbornadiene to quadricyclane is considered to be a TTET catalyzed reaction in most of the literature reports,[103] one study postulated a

https://doi.org/10.1021/jacs.1c11667
J. Am. Chem. Soc. 2022, 144, 963−976

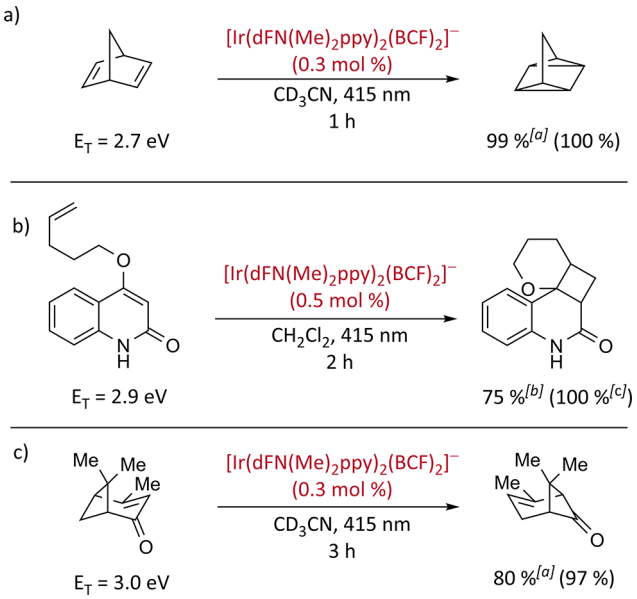

Figure 4. (a) [2 + 2] cycloaddition of norbornadiene to quadricyclane. (b) [2 + 2] cycloaddition of PQO to CQO. (c) [1,3] sigmatropic alkyl shift converting verbenone to chrysanthenone. [a]: ^{1}H NMR yield (conversion in parentheses) determined with the internal standard trimethyl(phenyl)silane. [b]: isolated yield. [c]: ^{1}H NMR conversion based on an NMR-scale experiment in CD_2Cl_2 after a reaction time of 90 min, determined using the internal standard trimethyl(phenyl)silane. The label "415 nm" indicates the use of a commercial LED with the spectral characteristics described in the main text.

partially redox-mediated mechanism via sensitization in a charge-transfer encounter complex and successfully employed an Ir(III)-based catalyst.[104] In our case, it seems plausible that the TTET pathway is operative.

Next, we explored a more challenging reaction, namely the intramolecular [2 + 2] cycloaddition of 4-(pent-4-en-1-yloxy)quinolin-2(1*H*)-one (PQO) to the corresponding cyclobutane product (CQO). The triplet energy (E_T) of PQO is 2.9 eV (Figure 4b), 0.2 eV above that of quadricyclane.[19,21] The reaction of PQO to CQO was completed after 90 min with 95% conversion based on a ^{1}H NMR experiment in CD_2Cl_2. The reaction was furthermore performed on the preparative scale in CH_2Cl_2 (0.7 mmol, 15 mg) and gave a 75% isolated yield after a reaction time of 2 h.

Finally, we turned our attention to an even more challenging reaction, the intramolecular [1,3] sigmatropic alkyl shift of verbenone to chrysanthenone (E_T of verbenone = 3.0 eV, Figure 4c).[1,105] Photoexcited $[Ir(dFN(Me)_2ppy)_2(BCF)_2]^-$ was able to catalyze this reaction with an 80% NMR-yield and a conversion of 97% after a reaction time of 3 h under irradiation with the 415 nm LED described above. The higher triplet energy of verbenone (3.0 eV) compared to PQO (2.9 eV) and norbornadiene (2.7 eV) results in less efficient TTET, which explains the need for a longer reaction time (3 h instead of 1−2 h on the NMR-scale).

The three experiments illustrated by Figure 4 demonstrate that $[Ir(dFN(Me)_2ppy)_2(BCF)_2]^-$ is well-suited for applications in demanding TTET catalysis and is able to sensitize substrates with triplet energies up to 3.0 eV. This is very uncommon for cyclometalated Ir(III) and other transition metal complexes.[1,2,14] Stern−Volmer luminescence quenching experiments with $[Ir(dFN(Me)_2ppy)_2(BCF)_2]^-$ and all three substrates from Figure 4 yielded rate constants ranging from 10^7 to 10^8 M^{-1} s^{-1} for TTET (Table S2). Control experiments in the absence of $[Ir(dFN(Me)_2ppy)_2(BCF)_2]^-$ were conducted for all three TTET catalyzed reactions and showed no detectable product formation after the indicated reaction times (Figures S45−S48).

Reductive Photocatalysis. As discussed in the section on the electrochemical properties above, the singly reduced $[Ir(dFN(Me)_2ppy)_2(BCF)_2]^{2-}$ complex is expected to be a powerful reductant (E^{red} = −2.42 V vs SCE, see Figure 2 and Table 1). Stern−Volmer experiments with triethylamine (TEA) demonstrate that the luminescent ^{3}MLCT/^{3}IL excited state of $[Ir(dFN(Me)_2ppy)_2(BCF)_2]^-$ is reductively quenched by TEA with a rate constant k_q of 1.7×10^5 M^{-1} s^{-1} (Figure S36). Even though this value is rather low, sufficiently high TEA concentrations in photocatalytic experiments are likely to favor a mechanism, in which reductive excited-state quenching by TEA predominates over direct electron transfer from excited $*[Ir(dFN(Me)_2ppy)_2(BCF)_2]^-$ to the substrate, particularly for substrates requiring reduction potentials more negative than −1.59 V vs SCE (see Figure 2). This is indeed the case for the substrates considered in the following.

In order to rule out possible complex degradation in the presence of TEA, we recorded UV−vis absorption spectra of $[Ir(dFN(Me)_2ppy)_2(BCF)_2]^-$ in the absence and the presence of 1000 equiv of TEA and obtained identical spectra even after letting the mixture stand for 20 min (Figure S29).

As first photoredox reactions, the debromination of 2-bromo-4-fluorobenzonitrile and the dechlorination of 2-chloro-4-fluorobenzonitrile were chosen (Figure 5a). Both substrates are known to require a reduction potential of at least ∼− 2.0 V vs SCE for reductive activation.[106] Fluoro-substituted substrates were employed for the convenient determination of the product yield and substrate conversion by ^{19}F-NMR, using 4-fluorotoluene as an internal standard. Photogenerated $[Ir(dFN(Me)_2ppy)_2(BCF)_2]^{2-}$ formed in the presence of 5 equiv of TEA was able to dehalogenate both substrates from Figure 5a after a reaction time of 6 h under irradiation with the above-mentioned 415 nm LED.

Having obtained these encouraging results, we decided to explore the photochemical deprotection of two tosyl-substituted compounds (Figure 5b). The ^{tBu}carbazole substrate (^{tBu}CBzTs, $E^{red} \approx -2.2$ V vs SCE, Figure S31) was successfully detosylated to ^{tBu}CBzH (Figure 5b, top) with high NMR yield (95%) and conversion (95%) after a reaction time of 3 h. In contrast, tosyl-protected pyrrole (PyrTs, $E^{red} \approx -2.1$ V vs SCE, Figure S31) proved to be a more challenging substrate (Figure 5b, bottom), even though it has a reduction potential similar to ^{tBu}CBzTs.

Lastly, the photochemical degradation of a lignin model compound was performed (Figure 5c). The degradation of lignin is of interest for the production of low molecular-weight aromatic compounds from biomass; however, conventional methods for this reaction are energy-intense, and therefore, significant efforts toward the photochemical lignin degradation were made in recent years.[107−112] After a reaction time of 2 h with $[Ir(dFN(Me)_2ppy)_2(BCF)_2]^-$ as photocatalyst and TEA as reductant, the reaction was complete and gave an NMR-yield of 93% and 66%, respectively, for the two degradation products (Figure 5c) and a substrate conversion of 100%. Control experiments in the absence of $[Ir(dFN(Me)_2ppy)_2(BCF)_2]^-$ were performed for all photoreductions and resulted

https://doi.org/10.1021/jacs.1c11667
J. Am. Chem. Soc. 2022, 144, 963−976

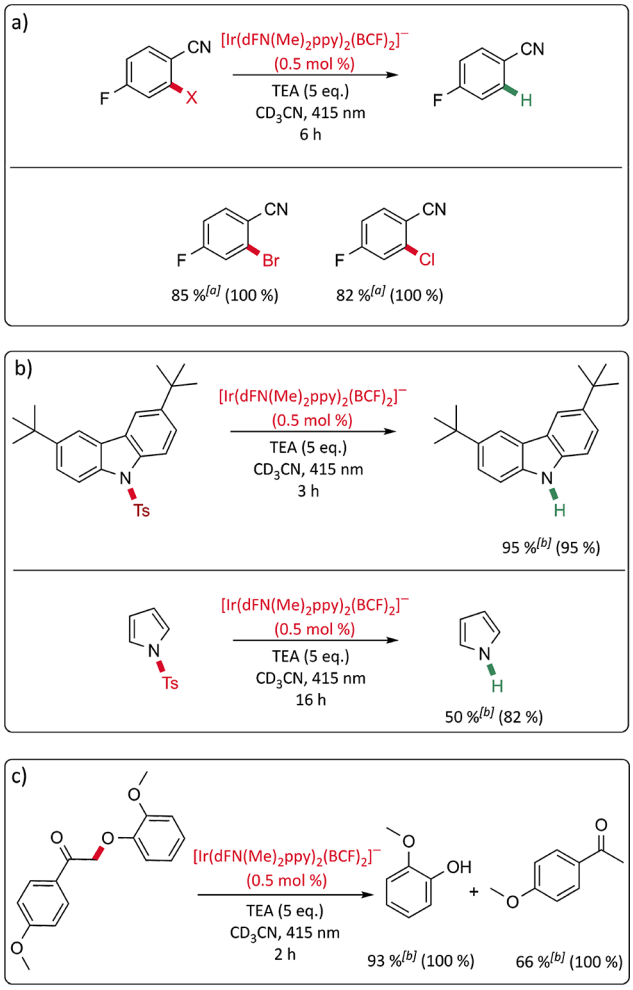

Figure 5. (a) Hydrodehalogenation of selected aryl halide substrates. (b) Detosylation of selected substrates. (c) Cleavage of a lignin model substrate. [a]: ^{19}F-NMR-yield (conversion in parentheses) determined with the internal standard 4-fluorotoluene. [b]: ^{1}H NMR-yield (conversion in parentheses) determined with the internal standard trimethyl(phenyl)silane. The label "415 nm" indicates the use of a commercial LED with the spectral characteristics described in the main text.

in only minor (<5%) product formation after the indicated reaction times (Figures S49–S58).

Sensitized Upconversion with a Biphenyl Annihilator. Given the high triplet energy of $[Ir(dFN(Me)_2ppy)_2(BCF)_2]^-$, we anticipated that it could be used to access highly energetic singlet excited states of organic fluorophores via triplet–triplet annihilation upconversion. Visible to UV-A (320–400 nm) upconversion has already been reported several times (see Introduction),[75−84] but reports of upconversion to the UV–B (280–320 nm) are very scarce.[83,85] A key reason for this is that the energy of the fluorescent singlet excited state reachable via upconversion is limited by the triplet energy of the sensitizers. In combination with $[Ir(dFN(Me)_2ppy)_2(BCF)_2]^-$, the 4,4′-di-*tert*-butyl-biphenyl (^{tBu}Bph) compound is a well-suited annihilator due to its high triplet energy of 2.84 eV and singlet-excited state energy of 4.25 eV (known values of unsubstituted biphenyl used as a proxy for ^{tBu}Bph here).[49] The twofold *tert*-butyl substitution of biphenyl seemed useful to limit aggregation and consequent excimer formation,[113] which is usually undesired in photochemical upconversion, because it lowers the overall energy conversion efficiency as a result of the lower photon energy emitted by the excimer compared to the monomer.[114]

Following excitation of the Ir(III) sensitizer at 355 nm, triplet–triplet energy transfer (TTET) to the ^{tBu}BPh annihilator occurs with a rate constant of $k_{TTET} = 9.8 \times 10^8$ M^{-1} s^{-1} based on a Stern–Volmer luminescence lifetime quenching experiment (Figure 6a). This rate constant is a factor of 19 below the diffusion limit in acetonitrile at 25 °C (1.9×10^{10} M^{-1} s^{-1}).[49] TTET rates typically approach the diffusion limit for driving-forces on the order of 0.2 eV or greater,[115] while for the $[Ir(dFN(Me)_2ppy)_2(BCF)_2]^-$/^{tBu}Bph donor–acceptor couple we estimate a driving-force of 0.15 eV based on the triplet energies of 2.99 and 2.84 eV. Given an inherent excited-state lifetime of 13.0 μs for the $[Ir(dFN(Me)_2ppy)_2(BCF)_2]^-$ sensitizer (Table 1), a ^{tBu}Bph concentration of 5.0 mM (as used below in the upconversion experiments) should therefore result in a TTET efficiency of 99%. Transient absorption spectroscopy confirms that the excited-state quenching by ^{tBu}Bph is due to TTET. Specifically, selective excitation of $[Ir(dFN(Me)_2ppy)_2(BCF)_2]^-$ (10^{-5} M) at 355 nm in the presence of ^{tBu}Bph (5.0 mM), results in a spectrum (Figure 6b) featuring a prominent absorption band with a maximum at 360 nm, which is attributable to triplet-excited ^{tBu}BPh due to its strong similarity to the characteristic absorption spectrum of unsubstituted triplet-excited biphenyl.[49] By analyzing the decay of this absorption signal, the rate constant for the first-order decay to the ^{tBu}BPh ground state ($k_T = 1.7 \times 10^4$ s^{-1}) and the second-order rate constant for the triplet–triplet-annihilation step ($k_{TTA} = 1.7 \times 10^{10}$ M^{-1} s^{-1}) can be calculated (see SI, page S35 for details).[116] The value for k_{TTA} is close to the diffusion limit in acetonitrile at 25 °C (1.9×10^{10} M^{-1} s^{-1}) and is in good agreement with literature values of comparable TTA systems.[106,116,117]

When a 10^{-5} M deaerated CH_3CN solution of [TBA][Ir(dFN(Me)$_2$ppy)$_2$(BCF)$_2$] containing 5.0 mM ^{tBu}Bph was irradiated with 405 nm light from a continuous wave (cw) laser, upconverted emission from singlet-excited ^{tBu}Bph was observed (Figure 6c). The band maximum of the delayed (upconverted) ^{tBu}Bph fluorescence is at 319 nm (3.89 eV), red-shifted by 0.07 eV compared to the maximum of the known fluorescence spectrum of unsubstituted biphenyl (313 nm) measured after direct UV excitation.[49] Though the anti-Stokes shift is in principle defined as the energy difference between absorption and corresponding emission band maxima, it has become rather common in the field of sensitized triplet–triplet annihilation upconversion to use the difference between the excitation wavelength and the maximum of the delayed fluorescence as a proxy for the anti-Stokes shift.[74,118−120] Using this simplistic approach, we calculate a pseudo anti-Stokes shift of 0.83 eV for our system (Figure 6d). The fluorescence band of ^{tBu}BPh under upconversion conditions features a main peak at 319 nm (solid vertical line in Figure 6c) including progression in an ~1400 cm^{-1} mode, leading to two shoulders at 306 and 333 nm (dashed vertical lines in Figure 6c). From the high-energy shoulder at 306 nm, the E_{00} energy of ^{tBu}BPh can be estimated and this analysis yields E_{00} = 4.05 eV. The values of 3.89 eV (for the band maximum) and 4.05 eV (for E_{00}) compare favorably to previously reported high-energy upconversion systems.[83,85]

In time-gated emission measurements under upconversion conditions, an additional emission band centered at 474 nm is observed after a time delay of 5 μs (Figure S37). We attribute

https://doi.org/10.1021/jacs.1c11667
J. Am. Chem. Soc. 2022, 144, 963−976

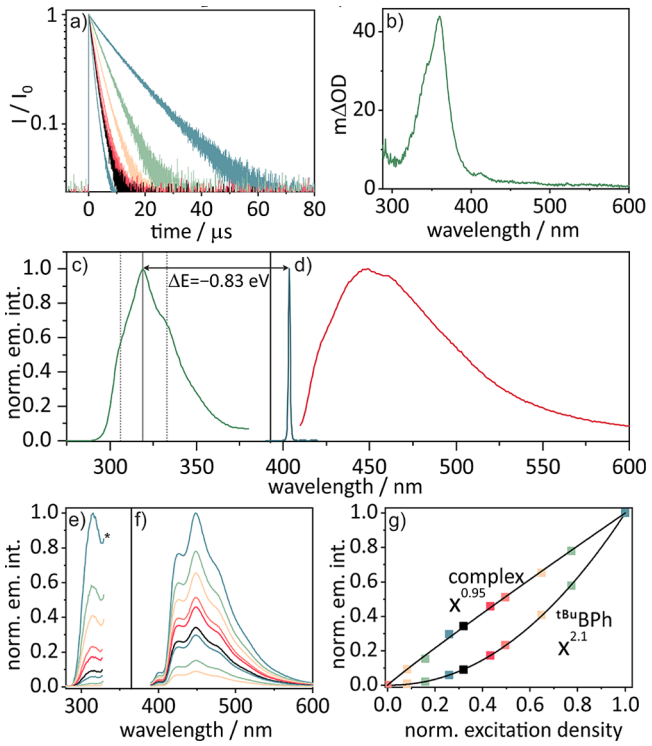

Figure 6. (a) Decay of $[Ir(dFN(Me)_2ppy)_2(BCF)_2]^-$ emission at 450 nm in the absence of ^{tBu}Bph (blue trace) and in the presence of increasing concentrations of ^{tBu}Bph (other traces) after 355 nm excitation of a 10^{-5} M [TBA]$[Ir(dFN(Me)_2ppy)_2(BCF)_2]$ solution in deaerated CH_3CN at 293 K. (b) Transient absorption spectrum measured after 355 nm excitation of a solution of [TBA]$[Ir(dFN(Me)_2ppy)_2(BCF)_2]$ (10^{-5} M) and ^{tBu}BPh (5.0 mM) in dry, deaerated CH_3CN at 293 K with laser pulses of ∼10 ns duration. The signals were time integrated over 200 ns with a time delay of 5 μs after the laser pulse. (c) Normalized upconversion emission of ^{tBu}BPh (5.0 mM) sensitized by $[Ir(dFN(Me)_2ppy)_2(BCF)_2]^-$ (10^{-5} M) in dry, deaerated CH_3CN at 293 K after excitation with a 405 nm cw laser. (d) Normalized prompt emission of the same 10^{-5} M solution of $[Ir(dFN(Me)_2ppy)_2(BCF)_2]^-$ as in (c), after excitation with a 405 nm cw laser, but without any ^{tBu}BPh (red), and the emission profile of the 405 nm cw laser (blue). Under these conditions, the emission band shows somewhat less fine structure; however, the emission band maximum is at the same position (448 nm) as in panel (f). (e) Normalized upconversion emission of ^{tBu}BPh (2.5 mM) sensitized by $[Ir(dFN(Me)_2ppy)_2(BCF)_2]^-$ (10^{-5} M) in dry, deaerated CH_3CN at 293 K using different excitation densities. The asterisk (*) marks the onset to an artifact caused by stray excitation light. (f) Normalized prompt emission of the same 10^{-5} M solution of $[Ir(dFN(Me)_2ppy)_2(BCF)_2]^-$ as in (e), but without any ^{tBu}BPh, using the same series of excitation densities as in (e). Excitation in (e) and (f) occurred at 355 nm with the internal lamp of the luminescence spectrometer. (g) Normalized peak emission intensities of ^{tBu}BPh and $[Ir(dFN(Me)_2ppy)_2(BCF)_2]^-$ as a function of the relative excitation density based on the spectra shown in (e) and (f). The black lines represent the best fits to a power function of the type $f(x) = y + a \cdot x^b$. The exponent b of the optimal fits of both the prompt Ir(III) complex emission intensity and the delayed ^{tBu}BPh fluorescence intensity is indicated in the figure.

this to delayed emission from $[Ir(dFN(Me)_2ppy)_2(BCF)_2]^-$ caused either by reverse energy transfer from triplet-excited ^{tBu}BPh, or by reabsorption of the upconverted light by $[Ir(dFN(Me)_2ppy)_2(BCF)_2]^-$, or a combination of both effects. Reverse (and uphill) TTET commonly occurs between donor−acceptor systems in which the triplet energies are fairly close.[121]

Photochemical upconversion with the $[Ir(dFN(Me)_2ppy)_2(BCF)_2]^-$ (10^{-5} M)/^{tBu}Bph (2.5 mM) donor−acceptor couple could also be achieved using the internal lamp of a luminescence spectrometer with an excitation wavelength of 355 nm (Figure 6e). The upconverted emission intensity under these conditions as a function of excitation density (Figure 6g) was fitted to a power function of the type $f(x) = y + a \cdot x^b$ and resulted in b = 2.1, confirming the expected biphotonic nature of the upconversion process.[122] In contrast, when a CH_3CN solution of $[Ir(dFN(Me)_2ppy)_2(BCF)_2]^-$ in the absence of ^{tBu}BPh is excited under the same conditions (Figure 6f), a linear dependence of the emission intensity on the excitation density is observed, and fitting to the same power function yields b = 0.95 (Figure 6g), in line with a monophotonic process. The low power density of the internal lamp of the luminescence spectrometer (compared to above-mentioned cw laser) has the advantage that the quadratic dependence of the upconverted emission intensity is observed much more readily compared to when higher excitation densities are employed.

The upconversion luminescence quantum yield Φ_{UC} was determined relative to the unquenched sensitizer emission and amounts to 0.07% (with a maximal theoretical limit of 50%)[123] under 405 nm excitation with a cw laser (Figure S40). Even though this value seems low, it should be noted that photochemical upconversion to the UV is often inefficient.[77,81,83] A few exceptions exceed Φ_{UC} = 5% based on nanocrystal photosensitizers,[84,124] and one example based on the combination of an Ir(III) sensitizer with TIPS-naphthalene (TIPS = 1,4-bis((triisopropylsilyl)ethynyl)) reached a record value of Φ_{UC} = 20%, though in this case the delayed fluorescence peaked at substantially longer wavelength (350 instead of 319 nm).[75,125]

Photostability. Photostability is an important aspect for many photophysical and photochemical applications. Previous studies of cyclometalated Ir(III) complexes demonstrated that this compound class can be relatively photorobust, particularly in the case of homoleptic tris(cyclometalated) variants, though systematic investigations seem to be scarce.[83,126,127] Isocyanoborato ligands recently provided Ru(II) complexes with remarkable photostability, and against this background it seemed meaningful to explore how stable the $[Ir(dFN(Me)_2ppy)_2(BCF)_2]^-$ complex is under visible light irradiation.[65] For this purpose, we employed ^{1}H NMR spectroscopy and followed the integrals of the aromatic signals of $[Ir(dFN(Me)_2ppy)_2(BCF)_2]^-$ (0.3 mM in CD_3CN) under high-power 415 nm irradiation (5.8 W) over the course of 60 min, once in neat solution and once in the presence of 60 mM norbornadiene as a triplet acceptor. In the presence of norbornadiene, no significant change in the integrals of the NMR signals can be observed up to t = 45 min (upper trace in Figure 7) and the Ir(III) complex evidently remains largely intact. In contrast, when the neat solution of [TBA]$[Ir(dFN(Me)_2ppy)_2(BCF)_2]$ was irradiated under identical conditions, there is clear evidence for photodegradation as the NMR signals gradually disappeared and became barely detectable after 60 min (lower trace in Figure 7; see SI, page S37 for details).

Evidently, the inherent photostability of the $[Ir(dFN(Me)_2ppy)_2(BCF)_2]^-$ complex under these excitation conditions with particularly high photon flux (5.8 W) is rather

https://doi.org/10.1021/jacs.1c11667
J. Am. Chem. Soc. 2022, 144, 963−976

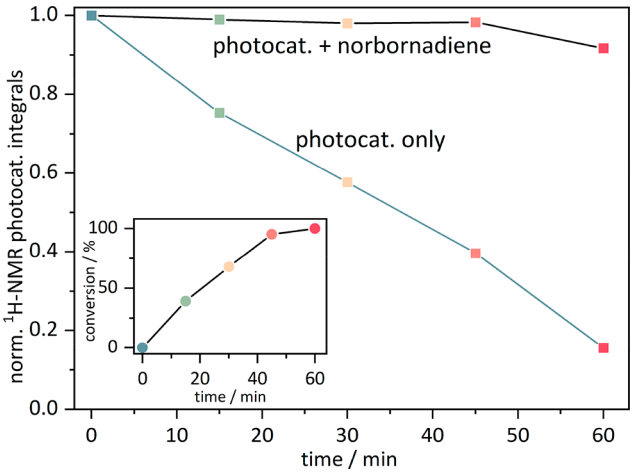

Figure 7. Main plot: photostability of 0.3 mM $[Ir(dFN(Me)_2ppy)_2(BCF)_2]^-$ in deaerated CD_3CN solutions upon irradiation with a 415 nm LED (5.8 W) in the presence and absence of 60 mM norbornadiene. Inset: conversion of norbornadiene to quadricyclane as a function of time in the same experiment.

modest, but improves considerably under conditions in which the photoactive excited state is deactivated rapidly by norbornadiene. It seems plausible that the comparatively long excited-state lifetime of $[Ir(dFN(Me)_2ppy)_2(BCF)_2]^-$ (13.0 μs) makes this complex more susceptible to photodegradation than luminophores with shorter excited-state lifetimes. For triplet harvesters in organic light emitting diodes, short-lived excited states are usually desirable exactly for this reason.[128−131] When a suitable substrate is present (which quenches the excited state and therefore shortens the excited-state lifetime of the photocatalyst), the photostability is significantly improved, as seen from the experiment with norbornadiene. Corroborating, the onset of photodegradation observed after 45 min in the presence of norbornadiene coincides with the completion of the photoisomerization reaction to quadricyclane, as seen from the inset in Figure 7. Evidently, as the substrate concentration decreases, quenching of the excited state becomes increasingly inefficient, and photodegradation sets in. The good photostability of $[Ir(dFN(Me)_2ppy)_2(BCF)_2]^-$ under catalytic (TTET) conditions is further substantiated by the fact that the conversion of norbornadiene to quadricyclane was performed with a catalyst loading of only 0.02%. Under these conditions, an NMR-yield of 92% was obtained after a reaction time of 8 h, corresponding to a turnover number (TON) > 4500.

CONCLUSIONS

Cyclometalated Ir(III) complexes are among the most frequently employed sensitizers for energy transfer[1,2,14,25−29] and photoredox catalysis;[31,132−136] and furthermore, they are of interest as triplet harvesters in organic light emitting diodes,[32,94,96,129,137−140] and as sensitizers for photochemical upconversion.[66,67,75−77,83] In many of these applications, the energy of the photoactive excited state of the Ir(III) complex is a crucial factor that can limit the scope of the sensitizer's applicability. Though cyclometalated Ir(III) complexes typically have their lowest electronically excited states at substantially higher energies than many other transition metal compounds, the most commonly employed Ir(III) complexes have excited state energies in the range 2.2 to 2.75 eV, too low for the applications demonstrated herein.[31] In this study, we have successfully applied a new strategy to reach the limit of 3.0 eV, based on the use of isocyanoborato strong-field π-acceptor ligands. This has opened new perspectives for applications in energy transfer catalysis and in triplet−triplet annihilation upconversion, as demonstrated by a series of light-driven reactions that crucially rely on a very high triplet energy and the very uncommon phenomenon of upconversion into the ultraviolet-B spectral range. The TTET-sensitized reactions accomplished with the Ir(III) isocyanoborato complex following excitation at the blue edge of the visible spectrum are unattainable with common Ir(III) photosensitizers, and to the best of our knowledge, there exists currently only one published example of upconversion to an excited state beyond 4 eV.[85] This illustrates how metal complex design can open the door to new photochemical and photophysical reactivities, and thus complements recent work on new photoactive coordination compounds with relevance to applications in preparative (organic) photochemistry and photochemical upconversion.[132,141−149]

The isocyanoborato ligand strategy furthermore provides access to a one-electron reduced form of the Ir(III) complex, which acts as a potent reductant (−2.42 V vs SCE), applicable to a range of challenging photoreductions including dehalogenations, detosylations, and the degradation of a lignin model substrate. This one-electron reduced form is accessible via reductive quenching of the photoactive excited state with tertiary amines, a process, which for other heteroleptic Ir(III) complexes induced reduction of an α-diimine ligand, leading to a new type of complex, which is likely the key catalytically active species in many iridium-catalyzed photoreductions.[150] The isocyanoborato π-acceptor ligands seem to lead to a comparatively stable one-electron reduced form of the Ir(III) complex, which directly engages in productive (single electron transfer) reactions with suitable substrates, rather than undergoing other conversions that obscure the overall reaction mechanism. Furthermore, the isocyanoborato coordination environment leads to good photostability under TTET catalysis conditions, in which the photoactive excited state reacts rapidly with triplet acceptors. In this context, our study illustrates the important difference between the inherent photostability of a compound (in the absence of any reaction partners), and its photostability under photochemical operation, in the presence of substrates. Likely due to the long excited-state lifetime of 13.0 μs, the inherent photostability of our Ir(III) isocyanoborato complex is substantially lower than that of two recently investigated Ru(II) isocyanoborato congeners, which exhibited much shorter excited-state lifetimes of 8.6 ns and 1.04 μs. This observation (following a well-known design principle of triplet-harvesting luminophores in organic light emitting diodes)[129,151] suggests that the types of very short-lived photoactive charge-transfer excited states, which are typically accessible in open-shell first-row transition metal complexes,[35,36,147,152−160] could in fact be rather photostable.

Isocyanoborato complexes of many different transition metal complexes are in principle synthetically amenable.[51−65] With the borylation reaction occurring in the second coordination sphere, this key step can be seen as a "late-stage modification" of cyanido precursor complexes with known photophysical and photochemical properties. This should simplify the rational development of many more isocyanoborato complexes with tailor-made photochemical properties, as illustrated herein on

https://doi.org/10.1021/jacs.1c11667
J. Am. Chem. Soc. 2022, 144, 963−976

the example of an Ir(III) complex. New types of photoactive isocyanoborato complexes could therefore open the door to further advances in organic (triplet) excited-state chemistry,[14,28,106,117,161−165] artificial photosynthesis,[166−170] and sensing.[171−173]

■ ASSOCIATED CONTENT

Supporting Information

The Supporting Information is available free of charge at https://pubs.acs.org/doi/10.1021/jacs.1c11667.

Synthetic protocols and characterization data, electrochemical characterization, equipment and methods, NMR data, details to photostability studies and upconversion measurements (PDF)

■ AUTHOR INFORMATION

Corresponding Author

Oliver S. Wenger − *Department of Chemistry, University of Basel, 4056 Basel, Switzerland;* orcid.org/0000-0002-0739-0553; Email: oliver.wenger@unibas.ch

Authors

Lucius Schmid − *Department of Chemistry, University of Basel, 4056 Basel, Switzerland;* orcid.org/0000-0001-5803-6979

Felix Glaser − *Department of Chemistry, University of Basel, 4056 Basel, Switzerland*

Raoul Schaer − *Department of Chemistry, University of Basel, 4056 Basel, Switzerland*

Complete contact information is available at: https://pubs.acs.org/10.1021/jacs.1c11667

Funding

This work was funded by the Swiss National Science Foundation through Grant Number 200021_178760.

Notes

The authors declare no competing financial interest.

■ REFERENCES

(1) Strieth-Kalthoff, F.; Glorius, F. Triplet Energy Transfer Photocatalysis: Unlocking the Next Level. *Chem.* **2020**, *6*, 1888−1903.

(2) Strieth-Kalthoff, F.; James, M. J.; Teders, M.; Pitzer, L.; Glorius, F. Energy transfer catalysis mediated by visible light: principles, applications, directions. *Chem. Soc. Rev.* **2018**, *47*, 7190−7202.

(3) Yoo, W.-J.; Tsukamoto, T.; Kobayashi, S. Visible Light-Mediated Ullmann-Type C-N Coupling Reactions of Carbazole Derivatives and Aryl Iodides. *Org. Lett.* **2015**, *17*, 3640−3642.

(4) Heitz, D. R.; Tellis, J. C.; Molander, G. A. Photochemical Nickel-Catalyzed C-H Arylation: Synthetic Scope and Mechanistic Investigations. *J. Am. Chem. Soc.* **2016**, *138*, 12715−12718.

(5) Sun, Z.; Kumagai, N.; Shibasaki, M. Photocatalytic α-Acylation of Ethers. *Org. Lett.* **2017**, *19*, 3727−3730.

(6) Kim, T.; McCarver, S. J.; Lee, C.; MacMillan, D. W. C. Sulfonamidation of Aryl and Heteroaryl Halides through Photosensitized Nickel Catalysis. *Angew. Chem., Int. Ed.* **2018**, *57*, 3488−3492.

(7) Ehrler, B.; Yanai, N.; Nienhaus, L. Up- and down-conversion in molecules and materials. *J. Chem. Phys.* **2021**, *154*, 070401.

(8) Ceroni, P. Energy Up-Conversion by Low-Power Excitation: New Applications of an Old Concept. *Chem.—Eur. J.* **2011**, *17*, 9560−9564.

(9) Molloy, J. J.; Schäfer, M.; Wienhold, M.; Morack, T.; Daniliuc, C. G.; Gilmour, R. Boron-enabled geometric isomerization of alkenes via selective energy-transfer catalysis. *Science* **2020**, *369*, 302−306.

(10) Singh, K.; Staig, S. J.; Weaver, J. D. Facile Synthesis of *Z* -Alkenes via Uphill Catalysis. *J. Am. Chem. Soc.* **2014**, *136*, 5275−5278.

(11) Metternich, J.; Gilmour, R. Photocatalytic E - Z Isomerization of Alkenes. *Synlett* **2016**, *27*, 2541−2552.

(12) Metternich, J. B.; Gilmour, R. A Bio-Inspired, Catalytic E - Z Isomerization of Activated Olefins. *J. Am. Chem. Soc.* **2015**, *137*, 11254−11257.

(13) Metternich, J. B.; Sagebiel, S.; Lückener, A.; Lamping, S.; Ravoo, B. J.; Gilmour, R. Covalent Immobilization of (−)-Riboflavin on Polymer Functionalized Silica Particles: Application in the Photocatalytic E-Z Isomerization of Polarized Alkenes. *Chem.—Eur. J.* **2018**, *24*, 4228−4233.

(14) Neveselý, T.; Wienhold, M.; Molloy, J. J.; Gilmour, R. Advances in the E → Z Isomerization of Alkenes Using Small Molecule Photocatalysts. *Chem. Rev.* **2021**. DOI: 10.1021/acs.chemrev.1c00324.

(15) Ma, J.; Strieth-Kalthoff, F.; Dalton, T.; Freitag, M.; Schwarz, J. L.; Bergander, K.; Daniliuc, C.; Glorius, F. Direct Dearomatization of Pyridines via an Energy-Transfer-Catalyzed Intramolecular [4 + 2] Cycloaddition. *Chem.* **2019**, *5*, 2854−2864.

(16) Hurtley, A. E.; Lu, Z.; Yoon, T. P. [2 + 2] Cycloaddition of 1,3-Dienes by Visible Light Photocatalysis. *Angew. Chem., Int. Ed.* **2014**, *53*, 8991−8994.

(17) Daub, M. E.; Jung, H.; Lee, B. J.; Won, J.; Baik, M.-H.; Yoon, T. P. Enantioselective [2 + 2] Cycloadditions of Cinnamate Esters: Generalizing Lewis Acid Catalysis of Triplet Energy Transfer. *J. Am. Chem. Soc.* **2019**, *141*, 9543−9547.

(18) Bach, T.; Bergmann, H.; Grosch, B.; Harms, K. Highly Enantioselective Intra- and Intermolecular [2 + 2] Photocycloaddition Reactions of 2-Quinolones Mediated by a Chiral Lactam Host: Host-Guest Interactions, Product Configuration, and the Origin of the Stereoselectivity in Solution. *J. Am. Chem. Soc.* **2002**, *124*, 7982−7990.

(19) Alonso, R.; Bach, T. A Chiral Thioxanthone as an Organocatalyst for Enantioselective [2 + 2] Photocycloaddition Reactions Induced by Visible Light. *Angew. Chem., Int. Ed.* **2014**, *53*, 4368−4371.

(20) Müller, C.; Bauer, A.; Maturi, M. M.; Cuquerella, M. C.; Miranda, M. A.; Bach, T. Enantioselective Intramolecular [2 + 2]-Photocycloaddition Reactions of 4-Substituted Quinolones Catalyzed by a Chiral Sensitizer with a Hydrogen-Bonding Motif. *J. Am. Chem. Soc.* **2011**, *133*, 16689−16697.

(21) Maturi, M. M.; Wenninger, M.; Alonso, R.; Bauer, A.; Pöthig, A.; Riedle, E.; Bach, T. Intramolecular [2 + 2] Photocycloaddition of 3- and 4-(But-3-enyl)oxyquinolones: Influence of the Alkene Substitution Pattern, Photophysical Studies, and Enantioselective Catalysis by a Chiral Sensitizer. *Chem.—Eur. J.* **2013**, *19*, 7461−7472.

(22) Murray, P. R. D.; Bussink, W. M. M.; Davies, G. H. M.; van der Mei, F. W.; Antropow, A. H.; Edwards, J. T.; D'Agostino, L. A.; Ellis, J. M.; Hamann, L. G.; Romanov-Michailidis, F.; Knowles, R. R. Intermolecular Crossed [2 + 2] Cycloaddition Promoted by Visible-Light Triplet Photosensitization: Expedient Access to Polysubstituted 2-Oxaspiro[3.3]heptanes. *J. Am. Chem. Soc.* **2021**, *143*, 4055−4063.

(23) Higgins, R. F.; Fatur, S. M.; Damrauer, N. H.; Ferreira, E. M.; Rappé, A. K.; Shores, M. P. Detection of an Energy-Transfer Pathway in Cr-Photoredox Catalysis. *ACS Catal.* **2018**, *8*, 9216−9225.

(24) Lu, Z.; Yoon, T. P. Visible Light Photocatalysis of [2 + 2] Styrene Cycloadditions by Energy Transfer. *Angew. Chem., Int. Ed.* **2012**, *124*, 10475−10478.

(25) Wearing, E. R.; Blackmun, D. E.; Becker, M. R.; Schindler, C. S. 1- and 2-Azetines via Visible Light-Mediated [2 + 2]-Cycloadditions of Alkynes and Oximes. *J. Am. Chem. Soc.* **2021**, *143*, 16235−16242.

(26) Teders, M.; Henkel, C.; Anhäuser, L.; Strieth-Kalthoff, F.; Gómez-Suárez, A.; Kleinmans, R.; Kahnt, A.; Rentmeister, A.; Guldi,

D.; Glorius, F. The energy-transfer-enabled biocompatible disulfide-ene reaction. *Nat. Chem.* **2018**, *10*, 981−988.
(27) Vasilopoulos, A.; Krska, S. W.; Stahl, S. S. C(sp^3)-H methylation enabled by peroxide photosensitization and Ni-mediated radical coupling. *Science* **2021**, *372*, 398−403.
(28) Becker, M. R.; Wearing, E. R.; Schindler, C. S. Synthesis of azetidines via visible-light-mediated intermolecular [2 + 2] photocycloadditions. *Nat. Chem.* **2020**, *12*, 898−905.
(29) Rykaczewski, K. A.; Schindler, C. S. Visible-Light-Enabled Paternò-Büchi Reaction via Triplet Energy Transfer for the Synthesis of Oxetanes. *Org. Lett.* **2020**, *22*, 6516−6519.
(30) Glaser, F.; Wenger, O. S. Recent progress in the development of transition-metal based photoredox catalysts. *Coord. Chem. Rev.* **2020**, *405*, 213129.
(31) Teegardin, K.; Day, J. I.; Chan, J.; Weaver, J. Advances in Photocatalysis: A Microreview of Visible Light Mediated Ruthenium and Iridium Catalyzed Organic Transformations. *Org. Process Res. Dev.* **2016**, *20*, 1156−1163.
(32) Mills, I. N.; Porras, J. A.; Bernhard, S. Judicious Design of Cationic, Cyclometalated Ir(III) Complexes for Photochemical Energy Conversion and Optoelectronics. *Acc. Chem. Res.* **2018**, *51*, 352−364.
(33) Bevernaegie, R.; Wehlin, S. A. M.; Piechota, E. J.; Abraham, M.; Philouze, C.; Meyer, G. J.; Elias, B.; Troian-Gautier, L. Improved Visible Light Absorption of Potent Iridium(III) Photo-oxidants for Excited-State Electron Transfer Chemistry. *J. Am. Chem. Soc.* **2020**, *142*, 2732−2737.
(34) Hockin, B. M.; Li, C.; Robertson, N.; Zysman-Colman, E. Photoredox Catalysts Based on Earth-Abundant Metal Complexes. *Catal. Sci. Technol.* **2019**, *9*, 889−915.
(35) Förster, C.; Heinze, K. Photophysics and photochemistry with Earth-abundant metals - fundamentals and concepts. *Chem. Soc. Rev.* **2020**, *49*, 1057−1070.
(36) Wegeberg, C.; Wenger, O. S. Luminescent First-Row Transition Metal Complexes. *JACS Au* **2021**, *1*, 1860−1876.
(37) DiLuzio, S.; Mdluli, V.; Connell, T. U.; Lewis, J.; VanBenschoten, V.; Bernhard, S. High-Throughput Screening and Automated Data-Driven Analysis of the Triplet Photophysical Properties of Structurally Diverse, Heteroleptic Iridium(III) Complexes. *J. Am. Chem. Soc.* **2021**, *143*, 1179−1194.
(38) Coppo, P.; Plummer, E. A.; De Cola, L. Tuning iridium(III) phenylpyridine complexes in the "almost blue" region. *Chem. Commun.* **2004**, 1774−1775.
(39) Münster, N.; Parker, N. A.; van Dijk, L.; Paton, R. S.; Smith, M. D. Visible Light Photocatalysis of 6π Heterocyclization. *Angew. Chem., Int. Ed.* **2017**, *56*, 9468−9472.
(40) Luis-Barrera, J.; Laina-Martín, V.; Rigotti, T.; Peccati, F.; Solans-Monfort, X.; Sodupe, M.; Mas-Ballesté, R.; Liras, M.; Alemán, J. Visible-Light Photocatalytic Intramolecular Cyclopropane Ring Expansion. *Angew. Chem., Int. Ed.* **2017**, *56*, 7826−7830.
(41) Zhu, M.; Xu, H.; Zhang, X.; Zheng, C.; You, S.-L. Visible-Light-Induced Intramolecular Double Dearomative Cycloaddition of Arenes. *Angew. Chem., Int. Ed.* **2021**, *60*, 7036−7040.
(42) Sajoto, T.; Djurovich, P. I.; Tamayo, A.; Yousufuddin, M.; Bau, R.; Thompson, M. E.; Holmes, R. J.; Forrest, S. R. Blue and near-UV phosphorescence from iridium complexes with cyclometalated pyrazolyl or N-heterocyclic carbene ligands. *Inorg. Chem.* **2005**, *44*, 7992−8003.
(43) Cañada, L. M.; Kölling, J.; Wen, Z.; Wu, J. I.-C.; Teets, T. S. Cyano-Isocyanide Iridium(III) Complexes with Pure Blue Phosphorescence. *Inorg. Chem.* **2021**, *60*, 6391−6402.
(44) Park, H. J.; Kim, J. N.; Yoo, H.-J.; Wee, K.-R.; Kang, S. O.; Cho, D. W.; Yoon, U. C. Rational Design, Synthesis, and Characterization of Deep Blue Phosphorescent Ir(III) Complexes Containing (4'-Substituted-2'-pyridyl)-1,2,4-triazole Ancillary Ligands. *J. Org. Chem.* **2013**, *78*, 8054−8064.
(45) Di Censo, D.; Fantacci, S.; De Angelis, F.; Klein, C.; Evans, N.; Kalyanasundaram, K.; Bolink, H. J.; Grätzel, M.; Nazeeruddin, M. K. Synthesis, Characterization, and DFT/TD-DFT Calculations of Highly Phosphorescent Blue Light-Emitting Anionic Iridium Complexes. *Inorg. Chem.* **2008**, *47*, 980−989.
(46) Pal, A. K.; Krotkus, S.; Fontani, M.; Mackenzie, C. F. R.; Cordes, D. B.; Slawin, A. M. Z.; Samuel, I. D. W.; Zysman-Colman, E. High-Efficiency Deep-Blue-Emitting Organic Light-Emitting Diodes Based on Iridium(III) Carbene Complexes. *Adv. Mater.* **2018**, *30*, 1804231.
(47) Paulisch, T. O.; Mai, L. A.; Strieth-Kalthoff, F.; James, M. J.; Henkel, C.; Guldi, D. M.; Glorius, F. Dynamic kinetic sensitization of β-dicarbonyl compounds - Access to medium-sized rings via a De Mayo-type ring expansion. *Angew. Chem., Int. Ed.* **2022**. DOI: 10.1002/anie.202112695.
(48) Wagner, P. J.; Waite, C. I. Photoinduced Radical Cleavage of Iodobenzophenones. *J. Phys. Chem.* **1995**, *99*, 7388−7394.
(49) Montalti, M.; Credi, A.; Prodi, L.; Gandolfi, M. T. *Handbook of Photochemistry*; 3rd ed.; CRC/Taylor & Francis: Boca Raton, FL, 2006.
(50) Nazeeruddin, M. K.; Humphry-Baker, R.; Berner, D.; Rivier, S.; Zuppiroli, L.; Graetzel, M. Highly Phosphorescence Iridium Complexes and Their Application in Organic Light-Emitting Devices. *J. Am. Chem. Soc.* **2003**, *125*, 8790−8797.
(51) Chan, K.-C.; Chu, W.-K.; Yiu, S.-M.; Ko, C.-C. Synthesis, characterization, photophysics and electrochemical study of luminescent iridium(III) complexes with isocyanoborate ligands. *Dalton Trans.* **2015**, *44*, 15135−15144.
(52) Chu, W. K.; Wei, X. G.; Yiu, S. M.; Ko, C. C.; Lau, K. C. Strongly Phosphorescent Neutral Rhenium(I) Isocyanoborato Complexes: Synthesis, Characterization, and Photophysical, Electrochemical, and Computational studies. *Chem.—Eur. J.* **2015**, *21*, 2603−2612.
(53) Chu, W.-K.; Ko, C.-C.; Chan, K.-C.; Yiu, S.-M.; Wong, F.-L.; Lee, C.-S.; Roy, V. A. L. A Simple Design for Strongly Emissive Sky-Blue Phosphorescent Neutral Rhenium Complexes: Synthesis, Photophysics, and Electroluminescent Devices. *Chem. Mater.* **2014**, *26*, 2544−2550.
(54) Chan, K. C.; Tong, K. M.; Cheng, S. C.; Ng, C. O.; Yiu, S. M.; Ko, C. C. Design of Luminescent Isocyano Rhenium(I) Complexes: Photophysics and Effects of the Ancillary Ligands. *Inorg. Chem.* **2018**, *57*, 13963−13972.
(55) Chakkaradhari, G.; Eskelinen, T.; Degbe, C.; Belyaev, A.; Melnikov, A. S.; Grachova, E. V.; Tunik, S. P.; Hirva, P.; Koshevoy, I. O. Oligophosphine-thiocyanate Copper(I) and Silver(I) Complexes and Their Borane Derivatives Showing Delayed Fluorescence. *Inorg. Chem.* **2019**, *58*, 3646−3660.
(56) Xiao, Y.; Chu, W.-K.; Ng, C.-O.; Cheng, S.-C.; Tse, M.-K.; Yiu, S.-M.; Ko, C.-C. Design and Synthesis of Luminescent Bis-(isocyanoborato) Rhenate(I) Complexes as a Selective Sensor for Cyanide Anion. *Organometallics* **2020**, *39*, 2135−2141.
(57) Chu, W.-K.; Yiu, S.-M.; Ko, C.-C. Neutral Luminescent Bis(bipyridyl) Osmium(II) Complexes with Improved Phosphorescent Properties. *Organometallics* **2014**, *33*, 6771−6777.
(58) Lancaster, S. J.; Walker, D. A.; Thornton-Pett, M.; Bochmann, M. New weakly coordinating counter anions for high activity polymerisation catalysts: $[(C_6F_5)_3B\text{-}CN\text{-}B(C_6F_5)_3]^-$ and $[Ni\{CNB(C_6F_5)_3\}_4]^{2-}$. *Chem. Commun.* **1999**, 1533−1534.
(59) Zhou, J.; Lancaster, S. J.; Walker, D. A.; Beck, S.; Thornton-Pett, M.; Bochmann, M. Synthesis, Structures, and Reactivity of Weakly Coordinating Anions with Delocalized Borate Structure: The Assessment of Anion Effects in Metallocene Polymerization Catalysts. *J. Am. Chem. Soc.* **2001**, *123*, 223−237.
(60) Na, H.; Maity, A.; Teets, T. S. Postsynthetic Systematic Electronic Tuning of Organoplatinum Photosensitizers via Secondary Coordination Sphere Interactions. *Organometallics* **2016**, *35*, 2267−2274.
(61) Chan, K.-C.; Cheng, S.-C.; Lo, L. T.-L.; Yiu, S.-M.; Ko, C.-C. Luminescent Charge-Neutral Copper(I) Phenanthroline Complexes with Isocyanoborate Ligand. *Eur. J. Inorg. Chem.* **2018**, *2018*, 897−903.

(62) Ngo, D. X.; Del Ciello, S. A.; Barth, A. T.; Hadt, R. G.; Grubbs, R. H.; Gray, H. B.; McNicholas, B. J. Electronic Structures, Spectroscopy, and Electrochemistry of $[M(diimine)(CN\text{-}BR_3)_4]^{2-}$ (M = Fe, Ru; R = Ph, C_6F_5) Complexes. *Inorg. Chem.* **2020**, *59*, 9594−9604.
(63) Ngo, D. X.; Del Ciello, S. A.; McNicholas, B. J.; Sanders, B. C.; Fajardo, J.; Gray, H. B.; Winkler, J. R. Cyano-ambivalence: Spectroscopy and photophysics of $[Ru(diimine)(CN\text{-}BR_3)_4]^{2-}$ complexes. *Polyhedron* **2020**, *188*, 114692.
(64) McNicholas, B. J.; Grubbs, R. H.; Winkler, J. R.; Gray, H. B.; Despagnet-Ayoub, E. Tuning the formal potential of ferrocyanide over a 2.1 V range. *Chem. Sci.* **2019**, *10*, 3623−3626.
(65) Schmid, L.; Kerzig, C.; Prescimone, A.; Wenger, O. S. Photostable Ruthenium(II) Isocyanoborato Luminophores and Their Use in Energy Transfer and Photoredox Catalysis. *JACS Au* **2021**, *1*, 819−832.
(66) Zhao, J.; Ji, S.; Guo, H. Triplet-triplet annihilation based upconversion: from triplet sensitizers and triplet acceptors to upconversion quantum yields. *RSC Adv.* **2011**, *1*, 937−950.
(67) Wang, J.; Lu, Y.; McCarthy, W.; Conway-Kenny, R.; Twamley, B.; Zhao, J.; Draper, S. M. Novel ruthenium and iridium complexes of N-substituted carbazole as triplet photosensitisers. *Chem. Commun.* **2018**, *54*, 1073−1076.
(68) Ravetz, B. D.; Pun, A. B.; Churchill, E. M.; Congreve, D. N.; Rovis, T.; Campos, L. M. Photoredox catalysis using infrared light via triplet fusion upconversion. *Nature* **2019**, *565*, 343−346.
(69) Imperiale, C. J.; Green, P. B.; Miller, E. G.; Damrauer, N. H.; Wilson, M. W. B. Triplet-Fusion Upconversion Using a Rigid Tetracene Homodimer. *J. Phys. Chem. Lett.* **2019**, *10*, 7463−7469.
(70) Rowe, J. M.; Zhu, J.; Soderstrom, E. M.; Xu, W.; Yakovenko, A.; Morris, A. J. Sensitized photon upconversion in anthracene-based zirconium metal-organic frameworks. *Chem. Commun.* **2018**, *54*, 7798−7801.
(71) Yanai, N.; Kimizuka, N. New Triplet Sensitization Routes for Photon Upconversion: Thermally Activated Delayed Fluorescence Molecules, Inorganic Nanocrystals, and Singlet-to-Triplet Absorption. *Acc. Chem. Res.* **2017**, *50*, 2487−2495.
(72) Gray, V.; Dzebo, D.; Abrahamsson, M.; Albinsson, B.; Moth-Poulsen, K. Triplet-triplet annihilation photon-upconversion: towards solar energy applications. *Phys. Chem. Chem. Phys.* **2014**, *16*, 10345−10352.
(73) Singh-Rachford, T. N.; Castellano, F. N. Photon upconversion based on sensitized triplet-triplet annihilation. *Coord. Chem. Rev.* **2010**, *254*, 2560−2573.
(74) Bilger, J. B.; Kerzig, C.; Larsen, C. B.; Wenger, O. S. A Photorobust Mo(0) Complex Mimicking $[Os(2,2'\text{-bipyridine})_3]^{2+}$ and Its Application in Red-to-Blue Upconversion. *J. Am. Chem. Soc.* **2021**, *143*, 1651−1663.
(75) Harada, N.; Sasaki, Y.; Hosoyamada, M.; Kimizuka, N.; Yanai, N. Discovery of Key TIPS-Naphthalene for Efficient Visible-to-UV Photon Upconversion under Sunlight and Room Light. *Angew. Chem., Int. Ed.* **2021**, *60*, 142−147.
(76) Zhao, W.; Castellano, F. N. Upconverted Emission from Pyrene and Di-tert-butylpyrene Using $Ir(ppy)_3$ as Triplet Sensitizer. *J. Phys. Chem. A* **2006**, *110*, 11440−11445.
(77) Duan, P.; Yanai, N.; Kimizuka, N. A bis-cyclometalated iridium complex as a benchmark sensitizer for efficient visible-to-UV photon upconversion. *Chem. Commun.* **2014**, *50*, 13111−13113.
(78) Chen, Q.; Liu, Y.; Guo, X.; Peng, J.; Garakyaraghi, S.; Papa, C. M.; Castellano, F. N.; Zhao, D.; Ma, Y. Energy Transfer Dynamics in Triplet-Triplet Annihilation Upconversion Using a Bichromophoric Heavy-Atom-Free Sensitizer. *J. Phys. Chem. A* **2018**, *122*, 6673−6682.
(79) Kawashima, Y.; Kouno, H.; Orihashi, K.; Nishimura, K.; Yanai, N.; Kimizuka, N. Visible-to-UV photon upconversion in air-saturated water by multicomponent co-assembly. *Mol. Syst. Des. Eng.* **2020**, *5*, 792−796.
(80) Barawi, M.; Fresno, F.; Pérez-Ruiz, R.; de la Peña O'Shea, V. A. Photoelectrochemical Hydrogen Evolution Driven by Visible-to-Ultraviolet Photon Upconversion. *ACS Appl. Energy Mater.* **2019**, *2*, 207−211.
(81) Singh-Rachford, T. N.; Castellano, F. N. Low Power Visible-to-UV Upconversion. *J. Phys. Chem. A* **2009**, *113*, 5912−5917.
(82) Yanai, N.; Kozue, M.; Amemori, S.; Kabe, R.; Adachi, C.; Kimizuka, N. Increased vis-to-UV upconversion performance by energy level matching between a TADF donor and high triplet energy acceptors. *J. Mater. Chem. C* **2016**, *4*, 6447−6451.
(83) Pfund, B.; Steffen, D. M.; Schreier, M. R.; Bertrams, M.-S.; Ye, C.; Börjesson, K.; Wenger, O. S.; Kerzig, C. UV Light Generation and Challenging Photoreactions Enabled by Upconversion in Water. *J. Am. Chem. Soc.* **2020**, *142*, 10468−10476.
(84) He, S.; Luo, X.; Liu, X.; Li, Y.; Wu, K. Visible-to-Ultraviolet Upconversion Efficiency above 10% Sensitized by Quantum-Confined Perovskite Nanocrystals. *J. Phys. Chem. Lett.* **2019**, *10*, 5036−5040.
(85) Zähringer, T. J. B.; Bertrams, M.-S.; Kerzig, C. Purely organic Vis-to-UV upconversion with an excited annihilator singlet beyond 4 eV. *J. Mater. Chem. C* **2022**. DOI: 10.1039/D1TC04782E.
(86) Tamayo, A. B.; Alleyne, B. D.; Djurovich, P. I.; Lamansky, S.; Tsyba, I.; Ho, N. N.; Bau, R.; Thompson, M. E. Synthesis and Characterization of Facial and Meridional Tris-cyclometalated Iridium(III) Complexes. *J. Am. Chem. Soc.* **2003**, *125*, 7377−7387.
(87) Brooks, J.; Babayan, Y.; Lamansky, S.; Djurovich, P. I.; Tsyba, I.; Bau, R.; Thompson, M. E. Synthesis and Characterization of Phosphorescent Cyclometalated Platinum Complexes. *Inorg. Chem.* **2002**, *41*, 3055−3066.
(88) Li, J.; Djurovich, P. I.; Alleyne, B. D.; Yousufuddin, M.; Ho, N. N.; Thomas, J. C.; Peters, J. C.; Bau, R.; Thompson, M. E. Synthetic Control of Excited-State Properties in Cyclometalated Ir(III) Complexes Using Ancillary Ligands. *Inorg. Chem.* **2005**, *44*, 1713−1727.
(89) Xia, J.-B.; Zhu, C.; Chen, C. Visible light-promoted metal-free sp^3-C-H fluorination. *Chem. Commun.* **2014**, *50*, 11701−11704.
(90) Turek, A. M.; Krishnamoorthy, G.; Phipps, K.; Saltiel, J. Resolution of Benzophenone Delayed Fluorescence and Phosphorescence with Compensation for Thermal Broadening. *J. Phys. Chem. A* **2002**, *106*, 6044−6052.
(91) Iqbal, N.; Choi, S.; You, Y.; Cho, E. J. Aerobic oxidation of aldehydes by visible light photocatalysis. *Tetrahedron Lett.* **2013**, *54*, 6222−6225.
(92) Singh, A.; Teegardin, K.; Kelly, M.; Prasad, K. S.; Krishnan, S.; Weaver, J. D. Facile Synthesis and Complete Characterization of Homoleptic and Heteroleptic Cyclometalated Iridium(III) Complexes for Photocatalysis. *J. Organomet. Chem.* **2015**, *776*, 51−59.
(93) Henwood, A. F.; Zysman-Colman, E. Lessons learned in tuning the optoelectronic properties of phosphorescent iridium(III) complexes. *Chem. Commun.* **2017**, *53*, 807−826.
(94) Lamansky, S.; Djurovich, P.; Murphy, D.; Abdel-Razzaq, F.; Lee, H.-E.; Adachi, C.; Burrows, P. E.; Forrest, S. R.; Thompson, M. E. Highly Phosphorescent Bis-Cyclometalated Iridium Complexes: Synthesis, Photophysical Characterization, and Use in Organic Light Emitting Diodes. *J. Am. Chem. Soc.* **2001**, *123*, 4304−4312.
(95) Costa, R. D.; Ortí, E.; Bolink, H. J.; Monti, F.; Accorsi, G.; Armaroli, N. Luminescent Ionic Transition-Metal Complexes for Light-Emitting Electrochemical Cells. *Angew. Chem., Int. Ed.* **2012**, *51*, 8178−8211.
(96) Lowry, M. S.; Bernhard, S. Synthetically Tailored Excited States: Phosphorescent, Cyclometalated Iridium(III) Complexes and Their Applications. *Chem.—Eur. J.* **2006**, *12*, 7970−7977.
(97) Indelli, M. T.; Bignozzi, C. A.; Marconi, A.; Scandola, F. Ruthenium(II) 2,2′-bipyridine complexes containing methyl isocyanide ligands. Extreme effects of nonchromophoric ligands on excited-state properties. *J. Am. Chem. Soc.* **1988**, *110*, 7381−7386.
(98) Caspar, J. V.; Meyer, T. J. Application of the energy gap law to nonradiative, excited-state decay. *J. Phys. Chem.* **1983**, *87*, 952−957.
(99) Helms, A. M.; Caldwell, R. A. Triplet Species from Norbornadiene. Time-Resolved Photoacoustic Calorimetry and ab Initio Studies of Energy, Geometry, and Spin-Orbit Coupling. *J. Am. Chem. Soc.* **1995**, *117*, 358−361.

(100) Gray, V.; Lennartson, A.; Ratanalert, P.; Börjesson, K.; Moth-Poulsen, K. Diaryl-substituted norbornadienes with red-shifted absorption for molecular solar thermal energy storage. *Chem. Commun.* **2014**, *50*, 5330−5332.
(101) Jevric, M.; Petersen, A. U.; Mansø, M.; Kumar Singh, S.; Wang, Z.; Dreos, A.; Sumby, C.; Nielsen, M. B.; Börjesson, K.; Erhart, P.; Moth-Poulsen, K. Norbornadiene-Based Photoswitches with Exceptional Combination of Solar Spectrum Match and Long-Term Energy Storage. *Chem.—Eur. J.* **2018**, *24*, 12767−12772.
(102) Orrego-Hernández, J.; Dreos, A.; Moth-Poulsen, K. Engineering of Norbornadiene/Quadricyclane Photoswitches for Molecular Solar Thermal Energy Storage Applications. *Acc. Chem. Res.* **2020**, *53*, 1478−1487.
(103) Arai, T.; Oguchi, T.; Wakabayashi, T.; Tsuchiya, M.; Nishimura, Y.; Oishi, S.; Sakuragi, H.; Tokumaru, K. Mechanistic Approach to the Sensitization Process of Aromatic Ketones in the Isomerization between Norbornadiene and Quadricyclane. *Bull. Chem. Soc. Jpn.* **1987**, *60*, 2937−2943.
(104) Grutsch, P. A.; Kutal, C. Charge-transfer sensitization of the valence photoisomerization of norbornadiene to quadricyclene by an orthometalated transition-metal complex. *J. Am. Chem. Soc.* **1986**, *108*, 3108−3110.
(105) Schuster, D. I.; Widman, D. The multiplicity of the [1,3]-sigmatropic photorearrangement of verbenone to chrysanthenone. *Tetrahedron Lett.* **1971**, *12*, 3571−3574.
(106) Glaser, F.; Kerzig, C.; Wenger, O. S. Sensitization-initiated electron transfer via upconversion: mechanism and photocatalytic applications. *Chem. Sci.* **2021**, *12*, 9922−9933.
(107) Nguyen, J. D.; Matsuura, B. S.; Stephenson, C. R. J. A Photochemical Strategy for Lignin Degradation at Room Temperature. *J. Am. Chem. Soc.* **2014**, *136*, 1218−1221.
(108) Zhou, Y.; Hu, D.; Li, D.; Jiang, X. Uranyl-Photocatalyzed Hydrolysis of Diaryl Ethers at Ambient Environment for the Directional Degradation of 4-O-5 Lignin. *JACS Au* **2021**, *1*, 1141−1146.
(109) Luo, J.; Zhang, X.; Lu, J.; Zhang, J. Fine Tuning the Redox Potentials of Carbazolic Porous Organic Frameworks for Visible-Light Photoredox Catalytic Degradation of Lignin β-O-4 Models. *ACS Catal.* **2017**, *7*, 5062−5070.
(110) Nguyen, S. T.; Murray, P. R. D.; Knowles, R. R. Light-Driven Depolymerization of Native Lignin Enabled by Proton-Coupled Electron Transfer. *ACS Catal.* **2020**, *10*, 800−805.
(111) Yoo, H.; Lee, M.-W.; Lee, S.; Lee, J.; Cho, S.; Lee, H.; Cha, H. G.; Kim, H. S. Enhancing Photocatalytic β-O-4 Bond Cleavage in Lignin Model Compounds by Silver-Exchanged Cadmium Sulfide. *ACS Catal.* **2020**, *10*, 8465−8475.
(112) Yabuta, T.; Hayashi, M.; Matsubara, R. Photocatalytic Reductive C-O Bond Cleavage of Alkyl Aryl Ethers by Using Carbazole Catalysts with Cesium Carbonate. *J. Org. Chem.* **2021**, *86*, 2545−2555.
(113) Ye, C.; Gray, V.; Kushwaha, K.; Kumar Singh, S.; Erhart, P.; Börjesson, K. Optimizing photon upconversion by decoupling excimer formation and triplet triplet annihilation. *Phys. Chem. Chem. Phys.* **2020**, *22*, 1715−1720.
(114) Ye, C.; Gray, V.; Mårtensson, J.; Börjesson, K. Annihilation Versus Excimer Formation by the Triplet Pair in Triplet-Triplet Annihilation Photon Upconversion. *J. Am. Chem. Soc.* **2019**, *141*, 9578−9584.
(115) Murtaza, Z.; Graff, D. K.; Zipp, A. P.; Worl, L. A.; Jones, W. E. J.; Bates, W. D.; Meyer, T. J. Energy Transfer in the Inverted Region: Calculation of Relative Rate Constants by Emission Spectral Fitting. *J. Phys. Chem.* **1994**, *98*, 10504−10513.
(116) Bachilo, S. M.; Weisman, R. B. Determination of Triplet Quantum Yields from Triplet-Triplet Annihilation Fluorescence. *J. Phys. Chem. A* **2000**, *104*, 7711−7714.
(117) Coles, M. S.; Quach, G.; Beves, J. E.; Moore, E. G. A Photophysical Study of Sensitization-Initiated Electron Transfer: Insights into the Mechanism of Photoredox Activity. *Angew. Chem., Int. Ed.* **2020**, *59*, 9522−9526.
(118) Nishimura, N.; Gray, V.; Allardice, J. R.; Zhang, Z.; Pershin, A.; Beljonne, D.; Rao, A. Photon Upconversion from Near-Infrared to Blue Light with TIPS-Anthracene as an Efficient Triplet-Triplet Annihilator. *ACS Materials Lett.* **2019**, *1*, 660−664.
(119) Haruki, R.; Sasaki, Y.; Masutani, K.; Yanai, N.; Kimizuka, N. Leaping across the visible range: near-infrared-to-violet photon upconversion employing a silyl-substituted anthracene. *Chem. Commun.* **2020**, *56*, 7017−7020.
(120) Sasaki, Y.; Amemori, S.; Kouno, H.; Yanai, N.; Kimizuka, N. Near infrared-to-blue photon upconversion by exploiting direct S-T absorption of a molecular sensitizer. *J. Mater. Chem. C* **2017**, *5*, 5063−5067.
(121) Strieth-Kalthoff, F.; Henkel, C.; Teders, M.; Kahnt, A.; Knolle, W.; Gómez-Suárez, A.; Dirian, K.; Alex, W.; Bergander, K.; Daniliuc, C. G.; Abel, B.; Guldi, D. M.; Glorius, F. Discovery of Unforeseen Energy-Transfer-Based Transformations Using a Combined Screening Approach. *Chem.* **2019**, *5*, 2183−2194.
(122) Haefele, A.; Blumhoff, J.; Khnayzer, R. S.; Castellano, F. N. Getting to the (Square) Root of the Problem: How to Make Noncoherent Pumped Upconversion Linear. *J. Phys. Chem. Lett.* **2012**, *3*, 299−303.
(123) Zhou, Y.; Castellano, F. N.; Schmidt, T. W.; Hanson, K. On the Quantum Yield of Photon Upconversion via Triplet-Triplet Annihilation. *ACS Energy Lett.* **2020**, *5*, 2322−2326.
(124) Gray, V.; Xia, P.; Huang, Z.; Moses, E.; Fast, A.; Fishman, D. A.; Vullev, V. I.; Abrahamsson, M.; Moth-Poulsen, K.; Lee Tang, M. CdS/ZnS core-shell nanocrystal photosensitizers for visible to UV upconversion. *Chem. Sci.* **2017**, *8*, 5488−5496.
(125) VanOrman, Z. A.; Nienhaus, L. Feeling blue no more: How TIPS-naphthalene enables efficient visible-to-UV upconversion. *Matter* **2021**, *4*, 2625−2626.
(126) Liu, C.; Lv, X.; Xing, Y.; Qiu, J. Trifluoromethyl-substituted cyclometalated iridium^{III} emitters with high photostability for continuous oxygen sensing. *J. Mater. Chem. C* **2015**, *3*, 8010−8017.
(127) Kerzig, C.; Guo, X.; Wenger, O. S. Unexpected Hydrated Electron Source for Preparative Visible-Light Driven Photoredox Catalysis. *J. Am. Chem. Soc.* **2019**, *141*, 2122−2127.
(128) Hamze, R.; Peltier, J. L.; Sylvinson, D.; Jung, M.; Cardenas, J.; Haiges, R.; Soleilhavoup, M.; Jazzar, R.; Djurovich, P. I.; Bertrand, G.; Thompson, M. E. Eliminating nonradiative decay in Cu(I) emitters: > 99% quantum efficiency and microsecond lifetime. *Science* **2019**, *363*, 601−606.
(129) Yersin, H.; Rausch, A. F.; Czerwieniec, R.; Hofbeck, T.; Fischer, T. The triplet state of organo-transition metal compounds. Triplet harvesting and singlet harvesting for efficient OLEDs. *Coord. Chem. Rev.* **2011**, *255*, 2622−2652.
(130) Zhang, Q.; Li, B.; Huang, S.; Nomura, H.; Tanaka, H.; Adachi, C. Efficient blue organic light-emitting diodes employing thermally activated delayed fluorescence. *Nat. Photonics* **2014**, *8*, 326−332.
(131) Ulbricht, C.; Beyer, B.; Friebe, C.; Winter, A.; Schubert, U. S. Recent Developments in the Application of Phosphorescent Iridium-(III) Complex Systems. *Adv. Mater.* **2009**, *21*, 4418−4441.
(132) Shon, J.-H.; Kim, D.; Rathnayake, M. D.; Sittel, S.; Weaver, J.; Teets, T. S. Photoredox catalysis on unactivated substrates with strongly reducing iridium photosensitizers. *Chem. Sci.* **2021**, *12*, 4069−4078.
(133) Shon, J.-H.; Teets, T. S. Potent Bis-Cyclometalated Iridium Photoreductants with β-Diketiminate Ancillary Ligands. *Inorg. Chem.* **2017**, *56*, 15295−15303.
(134) Prier, C. K.; Rankic, D. A.; MacMillan, D. W. C. Visible light photoredox catalysis with transition metal complexes: applications in organic synthesis. *Chem. Rev.* **2013**, *113*, 5322−5363.
(135) Zuo, Z.; Ahneman, D. T.; Chu, L.; Terrett, J. A.; Doyle, A. G.; MacMillan, D. W. C. Dual catalysis. Merging photoredox with nickel catalysis: coupling of α-carboxyl sp^3-carbons with aryl halides. *Science* **2014**, *345*, 437−440.
(136) Nguyen, J. D.; D'Amato, E. M.; Narayanam, J. M. R.; Stephenson, C. R. J. Engaging unactivated alkyl, alkenyl and aryl

iodides in visible-light-mediated free radical reactions. *Nat. Chem.* **2012**, *4*, 854−859.
(137) Hong, G.; Gan, X.; Leonhardt, C.; Zhang, Z.; Seibert, J.; Busch, J. M.; Bräse, S. A Brief History of OLEDs-Emitter Development and Industry Milestones. *Adv. Mater.* **2021**, *33*, 2005630.
(138) Kessler, F.; Watanabe, Y.; Sasabe, H.; Katagiri, H.; Nazeeruddin, M. K.; Grätzel, M.; Kido, J. High-performance pure blue phosphorescent OLED using a novel bis-heteroleptic iridium-(III) complex with fluorinated bipyridyl ligands. *J. Mater. Chem. C* **2013**, *1*, 1070−1075.
(139) Henwood, A. F.; Bansal, A. K.; Cordes, D. B.; Slawin, A. M. Z.; Samuel, I. D. W.; Zysman-Colman, E. Solubilised bright blue-emitting iridium complexes for solution processed OLEDs. *J. Mater. Chem. C* **2016**, *4*, 3726−3737.
(140) Tamayo, A. B.; Garon, S.; Sajoto, T.; Djurovich, P. I.; Tsyba, I. M.; Bau, R.; Thompson, M. E. Cationic bis-cyclometalated iridium-(III) diimine complexes and their use in efficient blue, green, and red electroluminescent devices. *Inorg. Chem.* **2005**, *44*, 8723−8732.
(141) Gernert, M.; Balles-Wolf, L.; Kerner, F.; Müller, U.; Schmiedel, A.; Holzapfel, M.; Marian, C. M.; Pflaum, J.; Lambert, C.; Steffen, A. Cyclic (Amino)(aryl)carbenes Enter the Field of Chromophore Ligands: Expanded π System Leads to Unusually Deep Red Emitting Cu^{I} Compounds. *J. Am. Chem. Soc.* **2020**, *142*, 8897−8909.
(142) Yam, V. W.-W.; Chan, A. K.-W.; Hong, E. Y.-H. Charge-transfer processes in metal complexes enable luminescence and memory functions. *Nat. Rev. Chem.* **2020**, *4*, 528−541.
(143) Kaufhold, S.; Imanbaew, D.; Riehn, C.; Rau, S. Rational *in situ* tuning of a supramolecular photocatalyst for hydrogen evolution. *Sustainable Energy Fuels* **2017**, *1*, 2066−2070.
(144) Zhang, Y.; Schulz, M.; Wächtler, M.; Karnahl, M.; Dietzek, B. Heteroleptic diimine-diphosphine Cu(I) complexes as an alternative towards noble-metal based photosensitizers: Design strategies, photophysical properties and perspective applications. *Coord. Chem. Rev.* **2018**, *356*, 127−146.
(145) Doettinger, F.; Yang, Y.; Schmid, M.-A.; Frey, W.; Karnahl, M.; Tschierlei, S. Cross-Coupled Phenyl- and Alkynyl-Based Phenanthrolines and Their Effect on the Photophysical and Electrochemical Properties of Heteroleptic Cu(I) Photosensitizers. *Inorg. Chem.* **2021**, *60*, 5391−5401.
(146) Sayre, H.; Ripberger, H. H.; Odella, E.; Zieleniewska, A.; Heredia, D. A.; Rumbles, G.; Scholes, G. D.; Moore, T. A.; Moore, A. L.; Knowles, R. R. PCET-Based Ligand Limits Charge Recombination with an Ir(III) Photoredox Catalyst. *J. Am. Chem. Soc.* **2021**, *143*, 13034−13043.
(147) Aydogan, A.; Bangle, R. E.; Cadranel, A.; Turlington, M. D.; Conroy, D. T.; Cauët, E.; Singleton, M. L.; Meyer, G. J.; Sampaio, R. N.; Elias, B.; Troian-Gautier, L. Accessing Photoredox Transformations with an Iron(III) Photosensitizer and Green Light. *J. Am. Chem. Soc.* **2021**, *143*, 15661−15673.
(148) Zhang, Y.; Lee, T. S.; Favale, J. M.; Leary, D. C.; Petersen, J. L.; Scholes, G. D.; Castellano, F. N.; Milsmann, C. Delayed Fluorescence from a Zirconium(IV) Photosensitizer with Ligand-to-Metal Charge-Transfer Excited States. *Nat. Chem.* **2020**, *12*, 345−352.
(149) Reichenauer, F.; Wang, C.; Förster, C.; Boden, P.; Ugur, N.; Báez-Cruz, R.; Kalmbach, J.; Carrella, L. M.; Rentschler, E.; Ramanan, C.; Niedner-Schatteburg, G.; Gerhards, M.; Seitz, M.; Resch-Genger, U.; Heinze, K. Strongly Red-Emissive Molecular Ruby $[Cr(bpmp)_2]^{3+}$ Surpasses $[Ru(bpy)_3]^{2+}$. *J. Am. Chem. Soc.* **2021**, *143*, 11843−11855.
(150) Connell, T. U.; Fraser, C. L.; Czyz, M. L.; Smith, Z. M.; Hayne, D. J.; Doeven, E. H.; Agugiaro, J.; Wilson, D. J. D.; Adcock, J. L.; Scully, A. D.; Gómez, D. E.; Barnett, N. W.; Polyzos, A.; Francis, P. S. The Tandem Photoredox Catalysis Mechanism of $[Ir(ppy)_2(dtb\text{-}bpy)]^{+}$ Enabling Access to Energy Demanding Organic Substrates. *J. Am. Chem. Soc.* **2019**, *141*, 17646−17658.
(151) To, W.-P.; Cheng, G.; Tong, G. S. M.; Zhou, D.; Che, C.-M. Recent Advances in Metal-TADF Emitters and Their Application in Organic Light-Emitting Diodes. *Front. Chem.* **2020**, *8*, 653.
(152) Woodhouse, M. D.; McCusker, J. K. Mechanistic Origin of Photoredox Catalysis Involving Iron(II) Polypyridyl Chromophores. *J. Am. Chem. Soc.* **2020**, *142*, 16229−16233.
(153) Dierks, P.; Päpcke, A.; Bokareva, O. S.; Altenburger, B.; Reuter, T.; Heinze, K.; Kühn, O.; Lochbrunner, S.; Bauer, M. Ground- and Excited-State Properties of Iron(II) Complexes Linked to Organic Chromophores. *Inorg. Chem.* **2020**, *59*, 14746−14761.
(154) Duchanois, T.; Liu, L.; Pastore, M.; Monari, A.; Cebrián, C.; Trolez, Y.; Darari, M.; Magra, K.; Francés-Monerris, A.; Domenichini, E.; Beley, M.; Assfeld, X.; Haacke, S.; Gros, P. NHC-Based Iron Sensitizers for DSSCs. *Inorganics* **2018**, *6*, 63.
(155) Kjær, K. S.; Kaul, N.; Prakash, O.; Chábera, P.; Rosemann, N. W.; Honarfar, A.; Gordivska, O.; Fredin, L. A.; Bergquist, K.-E.; Häggström, L.; Ericsson, T.; Lindh, L.; Yartsev, A.; Styring, S.; Huang, P.; Uhlig, J.; Bendix, J.; Strand, D.; Sundström, V.; Persson, P.; Lomoth, R.; Wärnmark, K. Luminescence and reactivity of a charge-transfer excited iron complex with nanosecond lifetime. *Science* **2019**, *363*, 249−253.
(156) Herr, P.; Kerzig, C.; Larsen, C. B.; Häussinger, D.; Wenger, O. S. Manganese(I) complexes with metal-to-ligand charge transfer luminescence and photoreactivity. *Nat. Chem.* **2021**, *13*, 956−962.
(157) Pal, A. K.; Li, C.; Hanan, G. S.; Zysman-Colman, E. Blue-Emissive Cobalt(III) Complexes and Their Use in the Photocatalytic Trifluoromethylation of Polycyclic Aromatic Hydrocarbons. *Angew. Chem., Int. Ed.* **2018**, *57*, 8027−8031.
(158) Wong, Y.-S.; Tang, M.-C.; Ng, M.; Yam, V. W.-W. Toward the Design of Phosphorescent Emitters of Cyclometalated Earth-Abundant Nickel(II) and Their Supramolecular Study. *J. Am. Chem. Soc.* **2020**, *142*, 7638−7646.
(159) Dorn, M.; Kalmbach, J.; Boden, P.; Kruse, A.; Dab, C.; Reber, C.; Niedner-Schatteburg, G.; Lochbrunner, S.; Gerhards, M.; Seitz, M.; Heinze, K. Ultrafast and long-time excited state kinetics of an NIR-emissive vanadium(III) complex I: synthesis, spectroscopy and static quantum chemistry. *Chem. Sci.* **2021**, *12*, 10780−10790.
(160) Wegeberg, C.; Häussinger, D.; Wenger, O. S. Pyrene-Decoration of a Chromium(0) Tris(diisocyanide) Enhances Excited State Delocalization: A Strategy to Improve the Photoluminescence of $3d^6$ Metal Complexes. *J. Am. Chem. Soc.* **2021**, *143*, 15800−15811.
(161) Crisenza, G. E. M.; Faraone, A.; Gandolfo, E.; Mazzarella, D.; Melchiorre, P. Catalytic asymmetric C-C cross-couplings enabled by photoexcitation. *Nat. Chem.* **2021**, *13*, 575−580.
(162) Cambié, D.; Dobbelaar, J.; Riente, P.; Vanderspikken, J.; Shen, C.; Seeberger, P. H.; Gilmore, K.; Debije, M. G.; Noël, T. Energy-Efficient Solar Photochemistry with Luminescent Solar Concentrator Based Photomicroreactors. *Angew. Chem., Int. Ed.* **2019**, *58*, 14374−14378.
(163) Zheng, J.; Swords, W. B.; Jung, H.; Skubi, K. L.; Kidd, J. B.; Meyer, G. J.; Baik, M.-H.; Yoon, T. P. Enantioselective Intermolecular Excited-State Photoreactions Using a Chiral Ir Triplet Sensitizer: Separating Association from Energy Transfer in Asymmetric Photocatalysis. *J. Am. Chem. Soc.* **2019**, *141*, 13625−13634.
(164) Poplata, S.; Tröster, A.; Zou, Y.-Q.; Bach, T. Recent Advances in the Synthesis of Cyclobutanes by Olefin [2 + 2] Photocycloaddition Reactions. *Chem. Rev.* **2016**, *116*, 9748−9815.
(165) Marzo, L.; Pagire, S. K.; Reiser, O.; König, B. Visible-Light Photocatalysis: Does It Make a Difference in Organic Synthesis? *Angew. Chem., Int. Ed.* **2018**, *57*, 10034−10072.
(166) Hammarström, L. Catalyst: Chemistry's Role in Providing Clean and Affordable Energy for All. *Chem.* **2016**, *1*, 515−518.
(167) Whittemore, T. J.; Xue, C.; Huang, J.; Gallucci, J. C.; Turro, C. Single-chromophore single-molecule photocatalyst for the production of dihydrogen using low-energy light. *Nat. Chem.* **2020**, *12*, 180−185.
(168) McCusker, J. K. Electronic structure in the transition metal block and its implications for light harvesting. *Science* **2019**, *363*, 484−488.
(169) Fang, X.; Kalathil, S.; Reisner, E. Semi-biological approaches to solar-to-chemical conversion. *Chem. Soc. Rev.* **2020**, *49*, 4926−4952.

https://doi.org/10.1021/jacs.1c11667
J. Am. Chem. Soc. 2022, 144, 963−976

(170) Lalrempuia, R.; McDaniel, N. D.; Müller-Bunz, H.; Bernhard, S.; Albrecht, M. Water Oxidation Catalyzed by Strong Carbene-Type Donor-Ligand Complexes of Iridium. *Angew. Chem., Int. Ed.* **2010**, *49*, 9765−9768.
(171) Heinemann, F.; Karges, J.; Gasser, G. Critical Overview of the Use of Ru(II) Polypyridyl Complexes as Photosensitizers in One-Photon and Two-Photon Photodynamic Therapy. *Acc. Chem. Res.* **2017**, *50*, 2727−2736.
(172) Lo, K. K.-W. Luminescent Rhenium(I) and Iridium(III) Polypyridine Complexes as Biological Probes, Imaging Reagents, and Photocytotoxic Agents. *Acc. Chem. Res.* **2015**, *48*, 2985−2995.
(173) Yang, C.; Mehmood, F.; Lam, T. L.; Chan, S. L.-F.; Wu, Y.; Yeung, C.-S.; Guan, X.; Li, K.; Chung, C. Y.-S.; Zhou, C.-Y.; Zou, T.; Che, C.-M. Stable luminescent iridium(III) complexes with bis(N-heterocyclic carbene) ligands: photo-stability, excited state properties, visible-light-driven radical cyclization and CO_2 reduction, and cellular imaging. *Chem. Sci.* **2016**, *7*, 3123−3136.

https://doi.org/10.1021/jacs.1c11667
J. Am. Chem. Soc. 2022, 144, 963−976